

9-1-2014

Synthesis of Homo- and Heterobimetallic $\text{Ni}^{\text{II}}-\text{M}^{\text{II}}$ (M = Fe, Co, Ni, Zn) Complexes Based on an Unsymmetric Ligand Framework: Structures, Spectroscopic Features, and Redox Properties

Denan Wang

Marquette University, denan.wang@marquette.edu

Sergey V. Lindeman

Marquette University, sergey.lindeman@marquette.edu

Adam T. Fiedler

Marquette University, adam.fiedler@marquette.edu

Synthesis of Homo- and Heterobimetallic Ni^{II}–M^{II} (M = Fe, Co, Ni, Zn) Complexes Based on an Unsymmetric Ligand Framework: Structures, Spectroscopic Features, and Redox Properties

Denan Wang

*Department of Chemistry, Marquette University,
Milwaukee, WI*

Sergey V. Lindeman

*Department of Chemistry, Marquette University,
Milwaukee, WI*

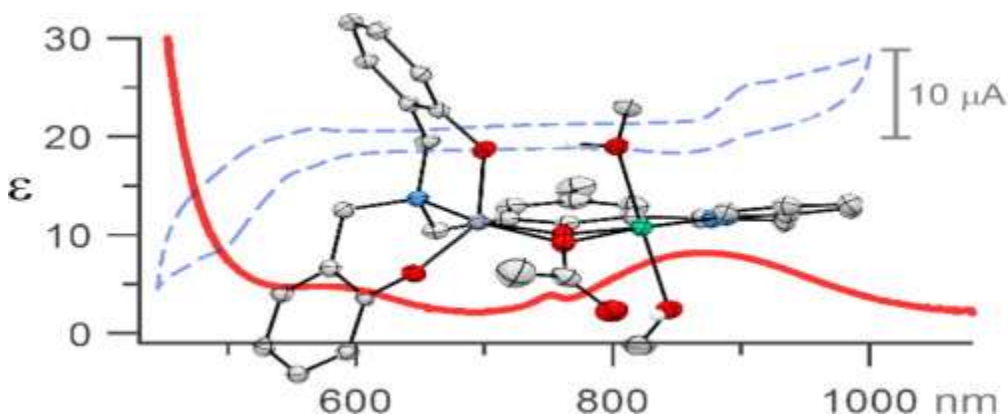
Adam T. Fiedler

*Department of Chemistry, Marquette University,
Milwaukee, WI*

Abstract: Several homo- and heterobimetallic Ni^{II}–M^{II} complexes (M^{II} = Fe, Co, Ni, Zn) supported by an unsymmetric polydentate ligand (**L**₁³⁻) are reported (**L**₁³⁻ is the trianion of 2-[bis(2-hydroxy-3,5-*tert*-

butylphenyl)aminomethyl]-4-methyl-6-[(2-pyridylmethyl)iminomethyl]phenol). The L_1^{3-} chelate provides two distinct coordination environments: a planar tridentate $\{N_2O\}$ site (**A**) and a tetradentate $\{NO_3\}$ site (**B**). Reaction of L_1^{3-} with equimolar amounts of Ni^{II} and M^{II} salts provides bimetallic complexes in which the Ni^{II} ion exclusively occupies the tetragonal **A**-site and the M^{II} ion is found in the tripodal **B**-site. X-ray crystal structures revealed that the two metal centers are bridged by the central phenolate donor of L_1^{3-} and an anionic X-ligand, where $X = \mu-1,1$ -acetate, hydroxide, or methoxide. The metal ions are separated by 3.0–3.1 Å in the $M_A M_B^X$ structures, where M_A and M_B indicate the ion located in the **A** and **B** sites, respectively, and X represents the second bridging ligand. Analysis of magnetic data and UV–Vis–NIR spectra indicate that, in all cases, the two metal ions adopt high-spin states in solution. The Ni_A^{II} centers undergo one-electron reduction at -1.17 V vs. SCE, while the Ni^{II} and Co^{II} ions in the phenolate-rich **B**-site are reduced at lower potentials. Significantly, the Ni_A^{II} center possesses three open or labile coordination sites in a meridional geometry, which are generally occupied by solvent-derived ligands in the crystal structures. The $Ni M_B^X$ complexes serve as structural mimics of heterometallic Ni-containing sites in biology, such as the C-cluster of carbon monoxide dehydrogenase (CODH).

Graphical abstract: The geometric and electronic structures of a series of Ni^{II} – M^{II} complexes ($M = Fe, Co, Ni, Zn$) featuring an unsymmetric chelate were characterized with crystallographic, spectroscopic, and electrochemical methods.

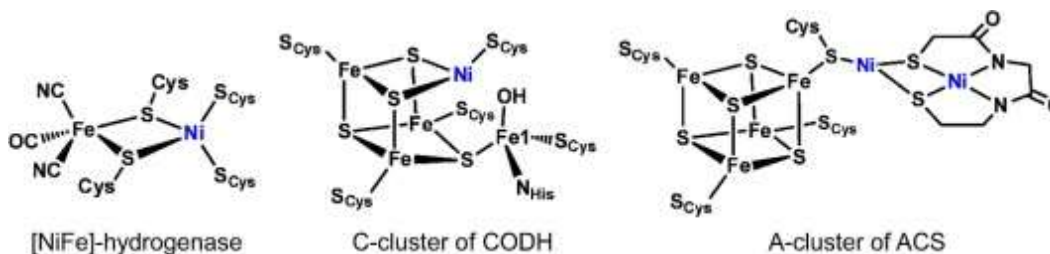


Keywords: Ni complexes, Heterobimetallic complexes, Electronic absorption spectroscopy, Electrochemistry

1. Introduction

Nickel centers in metalloenzymes are often embedded in polynuclear, heterometallic frameworks that facilitate the activation of small molecules via multiple electron and proton transfers.^{1;2} Three

examples are shown in Scheme 1. [NiFe]-hydrogenases feature an unusual heterobimetallic active site with a $[\text{NiFe}(\mu\text{-S}_{\text{Cys}})_2]$ core; in the available X-ray structures, the $\text{Ni}\cdots\text{Fe}$ distance ranges from 2.5 to 2.9 Å.^{3;4} While only the Ni site is redox-active under catalytic conditions, the Fe^{II} center is believed to play an important role in the binding and heterolytic bond cleavage of H_2 .^{5;6} The C-cluster of carbon monoxide dehydrogenase (CODH), shown in Scheme 1, catalyzes the reversible reaction: $\text{CO}_2 + 2\text{e}^- + 2\text{H}^+ \rightarrow \text{CO} + \text{H}_2\text{O}$.^{7;8} Based on crystallographic data, it appears that substrate binding and activation occurs at the heterobimetallic NiFe1 unit highlighted in Scheme 1,^{9;10;11;12} while the $[\text{Fe}_3\text{S}_4]$ component is only involved in shuttling electrons. The Fe1 center likely serves as a Lewis acid, stabilizing the critical NiCO_2Fe intermediate and facilitating cleavage of the CO bond. Finally, the A-cluster of acetyl-coenzyme A synthase (ACS) consists of a dinickel unit linked to a $[\text{Fe}_4\text{S}_4]$ cubane via a bridging cysteine residue. In each case, the presence of a metal center adjacent to the redox-active Ni site is critical for efficient catalysis.

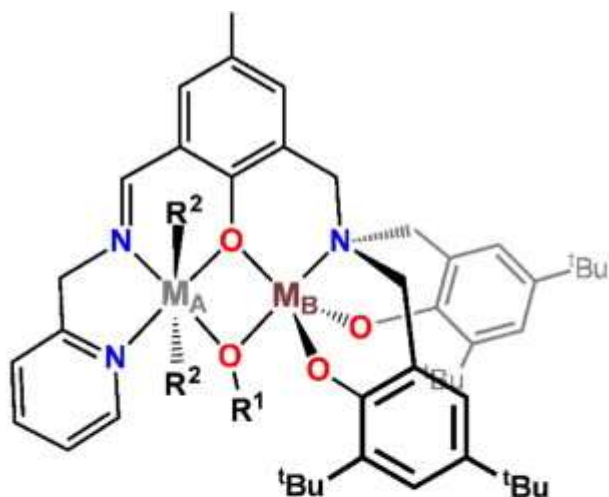


Scheme 1.

These biological precedents suggest that multinuclear Ni-containing complexes may have applications as synthetic catalysts for H_2 generation and CO_2 activation. In an effort to model the NiFe1 unit of the C-cluster, Holm and coworkers generated a series of bio-inspired complexes in which a Ni^{II} center is bound to a 2,6-pyridinedicarboxamidate pincer and a second M^{II} ion is coordinated to a pendant chelate ($\text{M} = \text{Mn}, \text{Fe}, \text{and Cu}$).^{13;14} The two metal centers are bridged by a single hydroxo, cyano, or formate ligand; for the hydroxo-bridged complexes, X-ray analysis revealed $\text{Ni}\cdots\text{M}$ distances near 3.7 Å and NiOM angles of $\sim 140^\circ$. More recently, Uyeda and Peters used a dimine-dioxime ligand to generate a heterobimetallic NiZn complex.¹⁵ The square-planar Ni^{II} center is linked to a $[\text{Zn}^{2+}(\text{Me}_3\text{-TACN})]$ unit via two oxime bridges ($\text{Me}_3\text{-TACN} = 1,4,7\text{-trimethyl-}1,4,7\text{-triazacyclononane}$). The addition of acetate or nitrite anions yielded

triply-bridged structures exhibiting Ni...Zn distances of ~ 3.45 Å. While numerous heterobimetallic NiM complexes (where M is a biologically-relevant transition metal) exist in the literature,^{16;17;18;19;20;21;22;23} their potential relevance to CODH and CO₂ reduction has not been explored.

In this manuscript, we report our initial efforts to generate homo- and heterobimetallic complexes containing a coordinatively unsaturated Ni^{II} center in close proximity to a second M^{II} site (M = Fe, Co, Ni, and Zn). Our studies have employed the unsymmetric ligand (**L**₁³⁻) shown in Scheme 2, which contains a central phenolate group capable of bridging the metal ions. Related ligands have been used to model the homo- and heterodinuclear active sites of various metalloenzymes.^{24;25;26} The **L**₁³⁻ ligand provides two distinct coordination environments: one bearing a Schiff-base moiety linked to a 2-pyridinylmethyl group (site **A**), and the other consisting of a tertiary amine with two additional phenolate donors (site **B**). Site **A** is well-suited for Ni^{II} coordination, while the trisphenolate site binds the second divalent metal ion. The phenolate-rich chelate is intended to depress the redox potentials of the metal centers, thereby enhancing the potential reactivity of the complexes towards electrophilic substrates, such as CO₂. X-ray crystal structures of the bimetallic complexes, described below, revealed that a second bridging ligand is also present: μ -1,1-acetate, hydroxide, or methoxide. As shown in Scheme 2, the series of complexes are labeled **M_AM_B^X**, where M_A and M_B identify the divalent ions located in the **A** and **B** sites, respectively, and **X** represents the second bridging ligand. The presence of two monoatomic bridging groups leads to short M_A^{II}-M_B^{II} distances of 3.0–3.1 Å. Both metal centers possess open or labile coordination sites for potential use in substrate binding and activation.



	M_A	M_B	R^1	R^2
NiFe^{OAc}	Ni ²⁺	Fe ²⁺	C(O)CH ₃	H ₂ O
NiCo^{OAc}	Ni ²⁺	Co ²⁺	C(O)CH ₃	MeOH
NiNi^{OAc}	Ni ²⁺	Ni ²⁺	C(O)CH ₃	MeOH
NiZn^{OAc}	Ni ²⁺	Zn ²⁺	C(O)CH ₃	MeOH
CoCo^{OAc}	Co ²⁺	Co ²⁺	C(O)CH ₃	MeOH
NiZn^{OH}	Ni ²⁺	Zn ²⁺	H	vacant
NiNi^{OMe}	Ni ²⁺	Ni ²⁺	CH ₃	MeOH

Scheme 2.

In addition to X-ray structural characterization, we have employed electrochemical and spectroscopic methods to analyze the electronic properties of the dinuclear complexes. Specifically, insights into the ligand-field environment were obtained using electronic absorption spectroscopy, and the redox potentials of the metal centers were probed with cyclic and square-wave voltammetry. Collectively, these results provide a foundation for future studies that will examine the reactivity of this new class of heterobimetallic complexes.

2. Experimental

2.1. Materials and physical methods

Reagents and solvents were purchased from commercial sources and used as received, unless otherwise noted. The air-sensitive complex **NiFe^{0Ac}** was synthesized and handled under inert atmosphere using a Vacuum Atmospheres Omni-Lab glovebox. Elemental analyses were performed at Midwest Microlab, LLC in Indianapolis, IN. Two instruments were used to measure electronic absorption spectra: an Agilent 8453 diode array spectrophotometer and an Agilent Cary 5000 UV-Vis-NIR spectrophotometer. Fourier-transform infrared (FTIR) spectra of solid samples were obtained with a Thermo Scientific Nicolet iS5 FTIR spectrometer equipped with the iD3 attenuated total reflectance accessory. ¹H and ¹³C NMR spectra were recorded at room temperature with a Varian 400 MHz spectrometer. Voltammetric measurements employed an epsilon EC potentiostat (iBAS) at a scan rate of 100 mV/s with 100 mM (NBu₄)PF₆ as the supporting electrolyte. The three-electrode cell contained a Ag/AgCl reference electrode, a platinum auxiliary electrode, and a glassy carbon working electrode. Potentials were referenced to the ferrocene/ferrocenium (Fc⁺⁰) couple, which has an *E*_{1/2} value of +0.45 V *versus* the standard calomel electrode (SCE) in DMF.²⁷ Solid-state magnetic susceptibility measurements were performed at room temperature using an AUTO balance manufactured by Sherwood Scientific. Solution-state magnetic moments were measured in chloroform using the Evans NMR method.

2.2. 3-(Bromomethyl)-2-hydroxy-5-methylbenzaldehyde (I)

Modifying a published procedure.²⁸ hydrobromic acid (30 mL, 47% in H₂O) was added to a mixture of 5-methylsalicylaldehyde (3.0 g, 22 mmol), paraformaldehyde (0.99 g, 33 mmol) and 10 drops of fuming sulfuric acid. The resulting solution was stirred at 70 °C for 6 h, resulting in formation of a white precipitate. After cooling to room temperature, the solid was isolated by filtration and washed with cold water (20 mL). The white product was dried under vacuum and used without further purification. Yield = 4.6 g, 91%. ¹H NMR (CDCl₃) δ: 2.34 (s, 3H), 4.55 (s, 2H), 7.33 (d, *J* = 1.4 Hz, 1H), 7.42 (d,

$J = 1.4$ Hz, 1H), 9.85 (s, 1H), 11.30 (s, 1H). ^{13}C NMR (CDCl_3) δ : 20.4, 26.9, 120.7, 126.2, 129.5, 134.4, 139.1, 157.7, 196.7.

2.3. Bis(3,5-di-*tert*-butyl-2-hydroxybenzyl)amine (II)²⁹

A mixture of 2,4-di-*tert*-butylphenol (2.0 g, 10 mmol) and hexamethylenetetramine (2.80 g, 20 mmol) was refluxed for 2 h in formic acid (100 mL, 85%). The reaction yielded crystals of the benzoxazine intermediate (1.85 g) that were subsequently isolated by filtration. This material was dissolved in ethylene glycol (100 mL) and hydrochloric acid (37%; 40 mL) and heated overnight at 130 °C. After cooling to room temperature, the hydrochloride salt of the desired product (i.e., **II**-HCl) was collected by filtration, washed with water, and dried under vacuum. The resulting solid was slowly added to a stirred mixture of aqueous KOH (1.8 M; 30 mL) and diethyl ether (50 mL). The organic layer was separated, dried over MgSO_4 , and the solvent removed under vacuum to give **II** as a pure white powder. Yield = 1.27 g, 56% overall. ^1H NMR (CDCl_3) δ : 1.30 (s, 18H), 1.46 (s, 18H), 3.93 (s, 4H), 6.97 (s, 2H), 7.26 (s, 2H). ^{13}C NMR (CDCl_3) δ : 29.8, 31.6, 34.2, 34.8, 51.4, 122.8, 123.5, 124.4, 135.9, 141.6, 152.6.

2.4. Compound III

3-(Bromomethyl)-2-hydroxy-5-methylbenzaldehyde (**I**, 2.14 g, 9.4 mmol) was added dropwise to a solution of bis(3,5-di-*tert*-butyl-2-hydroxybenzyl)amine (**II**; 4.24 g, 9.4 mmol) and triethylamine (2.6 mL, 19 mmol) in THF (50 mL). The mixture was refluxed overnight and then filtered to remove the salt byproduct. After evaporation of solvent under vacuum, the crude product was isolated as pale yellow solid. Purification by flash column chromatography (10:1 mixture of hexanes:EtOAc) provided **III** as a pure solid. Yield = 3.0 g, 53%. ^1H NMR (CDCl_3) δ : 1.28 (s, 18H), 1.35 (s, 18H), 2.23 (s, 3H), 3.70 (s, 2H), 3.74 (s, 4H), 6.95 (d, $J = 2.3$ Hz, 2H), 7.08 (s, 1H), 7.19 (d, $J = 2.3$ Hz, 2H), 7.24 (s, 1H), 9.83 (s, 1H). ^{13}C NMR (CDCl_3) δ : 20.1, 29.6, 31.7, 34.1, 34.9, 52.8, 58.2, 120.2, 121.8, 123.5, 125.0, 125.9, 129.2, 133.3, 135.9, 140.1, 141.3, 152.3, 158.1, 196.7.

2.5. Ligand L_1H_3

Modifying a published procedure,³⁰ 2-picolylamine (0.21 mL, 2.0 mmol) was added to a solution of compound **III** (1.2 g, 2.0 mmol) in methanol (20 mL). The mixture was refluxed overnight under argon, causing the color to change to yellow. Removal of solvent under vacuum provided L_1H_3 as yellow powder, which was used without further purification. Yield = 1.33 g, 96%. 1H NMR ($CDCl_3$) δ : 1.27 (s, 18H), 1.34 (s, 18H), 2.19 (s, 3H), 3.73 (s, 2H), 3.77 (s, 4H), 5.00 (s, 2H), 6.87 (s, 1H), 6.94 (d, $J = 2.3$ Hz, 2H), 7.00 (s, 1H), 7.18 (d, $J = 2.3$ Hz, 2H), 7.29 (dd, $J = 7.6, 5.0$ Hz, 1H), 7.48 (d, $J = 7.6$ Hz, 1H), 7.80 (t, $J = 7.6$ Hz, 1H), 8.24 (br s, 3H, OH), 8.40 (s, 1H), 8.61 (d, $J = 5.0$ Hz, 1H). ^{13}C NMR ($CDCl_3$) δ : 20.2, 29.6, 31.7, 34.1, 34.9, 54.0, 58.3, 63.9, 118.2, 122.0, 122.1, 122.7, 123.4, 124.9, 125.0, 127.8, 131.6, 135.5, 136.0, 138.0, 141.2, 148.4, 142.5, 157.6, 157.8, 167.3. FTIR (cm^{-1} , solid): 2951 (s), 2904 (m), 2866 (m), 1632 (m), 1590 (m).

2.6. General procedure for synthesis of $[NiM(L_1)(\mu-OAc)]$ complexes (NiM_B^{OAc})

The L_1H_3 ligand (300 mg, 0.434 mmol) and three equivalents of NaOMe (70 mg, 1.3 mmol) were stirred in MeOH (10 mL) for 10 min, followed by addition of $Ni(OAc)_2 \cdot 4H_2O$ (108 mg, 0.434 mmol) and one equivalent of the appropriate $M_B(OAc)_2$ salt. The mixture was stirred overnight and the solvent removed under vacuum. The resulting solid was taken up in THF and filtered through Celite to remove sodium salts. Evaporation of solvent provided the crude solid. The methods used to grow crystals of the complexes are described below.

2.7. $[NiFe(L_1)(\mu-OAc)]$ ($NiFe^{OAc}$)

X-ray quality crystals were obtained from a 1:1 mixture of acetone:MeCN. Yield: 40%. Material for elemental analysis was purified by recrystallization in a 1:1 mixture of MeCN and MeOH. *Anal.* Calc. for $C_{49}H_{69}FeN_3NiO_7$ ($M_W = 926.63$ g mol $^{-1}$): C, 63.51; H, 7.51; N, 4.53. Found: C, 63.48; H, 7.36; N, 4.80%. UV-Vis [λ_{max} , nm (ϵ , M $^{-1}$ cm $^{-1}$) in DMF]: 890 (18), 530 (1000). FTIR (cm^{-1} , solid): 2951

(s), 2902 (m), 2864 (m), 1621 (m), 1603 (m), 1573 (s, $\nu[\text{C}=\text{O}_{\text{OAc}}]$). $\mu_{\text{eff}} = 5.02 \mu_{\text{B}}$ (Evans method, CHCl_3).

2.8. $[\text{NiCo}(\text{L}_1)(\mu\text{-OAc})] (\text{NiCo}^{\text{OAc}})$

The crude solid was dissolved in a 1:1 mixture of MeCN and MeOH, which yielded orange crystals after several days. Yield: 60%. *Anal.* Calc. for $\text{C}_{49}\text{H}_{69}\text{CoN}_3\text{NiO}_7$ ($M_{\text{W}} = 929.71 \text{ g mol}^{-1}$): C, 63.30; H, 7.48; N, 4.52. Found: C, 63.66; H, 7.43; N, 4.81. UV-Vis-NIR [λ_{max} , nm (ϵ , $\text{M}^{-1} \text{ cm}^{-1}$) in DMF]: 1630 (6), 1050 (sh), 830 (7), 640 (sh), 580 (sh). FTIR (cm^{-1} , solid): 2951 (s), 2902 (m), 2864 (m), 1627 (w), 1605 (m), 1565 (s, $\nu[\text{C}=\text{O}_{\text{OAc}}]$). $\mu_{\text{eff}} = 4.51$ (solid state), $4.72 \mu_{\text{B}}$ (Evans method, CHCl_3).

2.9. $[\text{Ni}_2(\text{L}_1)(\mu\text{-OAc})] (\text{NiNi}^{\text{OAc}})$

Yellow crystals were grown from a concentrated solution in 1:1 MeCN:MeOH. Yield: 36%. *Anal.* Calc. for $\text{C}_{49}\text{H}_{69}\text{N}_3\text{Ni}_2\text{O}_7$ ($M_{\text{W}} = 929.47 \text{ g mol}^{-1}$): C, 63.32; H, 7.48; N, 4.52. Found: C, 62.52; H, 7.28; N, 4.84%. UV-Vis [λ_{max} , nm (ϵ , $\text{M}^{-1} \text{ cm}^{-1}$) in DMF]: 866 (17), 740 (19), 500 (sh). FTIR (cm^{-1} , solid): 2951 (s), 2903 (m), 2864 (m), 1625 (m), 1605 (s), 1585 (s, $\nu[\text{C}=\text{O}_{\text{OAc}}]$). $\mu_{\text{eff}} = 3.66$ (solid state), $3.82 \mu_{\text{B}}$ (Evans method, CHCl_3).

2.10. $[\text{NiZn}(\text{L}_1)(\mu\text{-OAc})] (\text{NiZn}^{\text{OAc}})$

The yellow solid was washed with cold MeOH, dissolved in CH_2Cl_2 , and layered with MeOH to provide X-ray quality crystals. Yield: 45%. *Anal.* Calc. for $\text{C}_{49}\text{H}_{69}\text{N}_3\text{NiO}_7\text{Zn}$ ($M_{\text{W}} = 936.16 \text{ g mol}^{-1}$): C, 62.87; H, 7.43; N, 4.49. Found: C, 62.67; H, 6.97; N, 4.62%. UV-vis [λ_{max} , nm (ϵ , $\text{M}^{-1} \text{ cm}^{-1}$) in DMF]: 869 (8), 575 (4). FTIR (cm^{-1} , solid): 2951 (s), 2902 (m), 2863 (m), 1643 (m), 1604 (s), 1586 (s, $\nu[\text{C}=\text{O}_{\text{OAc}}]$). $\mu_{\text{eff}} = 2.69$ (solid state), $2.67 \mu_{\text{B}}$ (Evans method, CHCl_3).

2.11. $[\text{Co}_2(\text{L}_1)(\mu\text{-OAc})] (\text{CoCo}^{\text{OAc}})$

Three equivalents of NaOMe (47 mg, 0.87 mmol) were added to a stirred solution of L_1H_3 (200 mg, 0.29 mmol) in MeOH (10 mL). After 10 min, two equivalents of $\text{Co}(\text{OAc})_2 \cdot 4\text{H}_2\text{O}$ (144 mg, 0.58 mmol) were

added and the resulting mixture was stirred overnight. The solvent was evaporated under vacuum and the crude material dissolved in THF (10 mL). After filtering through Celite to remove sodium salts, the THF solvent was evaporated to give a yellow solid that was taken up in a 1:1 mixture of MeCN:MeOH. X-ray-quality crystals appeared after a few days. Yield = 111 mg, 41%. *Anal.* Calc. for $C_{49}H_{69}Co_2N_3O_7$ ($M_W = 929.95 \text{ g mol}^{-1}$): C, 63.29; H, 7.48; N, 4.52. Found: C, 63.33; H, 7.40; N, 4.90%. UV-Vis-NIR [λ_{max} , nm (ϵ , $M^{-1} \text{ cm}^{-1}$) in DMF]: 1585 (5), 920 (3), 660 (sh), 580 (sh), 530 (sh). FTIR (cm^{-1} , solid): 2952 (s), 2902 (m), 2865 (m), 1626 (w), 1602 (m), 1568 (s, $\nu[C=O_{OAc}]$). $\mu_{eff} = 5.31 \mu_B$ (Evans method, $CHCl_3$).

2.12. $[NiZn(L_1)(\mu-OH)] (NiZn^{OH})$

The L_1H_3 ligand (300 mg, 0.434 mmol) and three equivalents of NEt_3 (0.18 mL, 1.3 mmol) were dissolved in MeOH (10 mL), followed by addition of equimolar amounts of $Ni(ClO_4)_2 \cdot 6H_2O$ (159 mg, 0.434 mmol) and $Zn(ClO_4)_2 \cdot 6H_2O$ (162 mg, 0.434 mmol). After stirring for one hour, one equivalent of $(NEt_4)OH$ (0.434 mL, 1.0 M solution in MeOH) was injected, resulting in formation of a light brown precipitate. The solid was collected and washed with cold methanol to provide the crude product as a yellow powder. X-ray-quality crystals were grown by vapor diffusion of pentane into a concentrated 1,2-dichloroethane (DCE) solution. Yield = 162 mg, 40%. *Anal.* Calc. for $C_{45}H_{59}N_3NiO_4Zn \cdot DCE$ ($M_W = 929.00 \text{ g mol}^{-1}$): C, 60.76; H, 6.84; N, 4.52. Found: C, 60.50; H, 7.02; N, 4.92%. UV-Vis [λ_{max} , nm (ϵ , $M^{-1} \text{ cm}^{-1}$) in DMF]: 848 (18), 510 (sh). FTIR (cm^{-1} , solid): 2949 (s), 2903 (m), 2864 (m), 1626 (m), 1601 (m), 1553 (w). $\mu_{eff} = 1.43$ (solid state), $2.53 \mu_B$ (Evans method, $CHCl_3$).

2.13. $[Ni_2(L_1)(\mu-OCH_3)] (NiNi^{OMe})$

$Ni(ClO_4)_2 \cdot 6H_2O$ (211 mg, 0.578 mmol) and triethylamine (121 mL, 0.867 mmol) were added to a solution of L_1H_3 (200 mg, 0.29 mmol) in 10 mL of MeOH. After one hour, a single equivalent of $(NEt_4)OH$ (0.29 mmol) was added. The mixture was stirred overnight, eventually giving rise to a dark yellow precipitate. The solvent was removed under vacuum, and the resulting solid was dissolved in THF. Insoluble salts were eliminated by filtration and the THF solvent was

removed to yield the crude brown product. X-ray-quality crystals were grown from a concentrated 1:1 solution of MeCN:MeOH.

Yield = 147 mg, 57%. *Anal.* Calc. for C₄₈H₆₉N₃Ni₂O₆ (*M_W* = 901.46 g mol⁻¹): C, 63.95; H, 7.72; N, 4.66. Found: C, 64.01; H, 7.68; N, 4.70%. UV-vis [λ_{max} , nm (ϵ , M⁻¹ cm⁻¹) in DMF]: 890 (20), 760 (25). FTIR (cm⁻¹, solid): 2950 (s), 2902 (m), 2865 (m), 1634 (w), 1604 (m), 1573 (w). μ_{eff} = 3.77 μ_{B} (Evans method, CHCl₃).

2.14. Crystallographic studies

X-ray diffraction (XRD) data were collected at 100 K with an Oxford Diffraction SuperNova kappa-diffractometer (Agilent Technologies) equipped with dual microfocus Cu/Mo X-ray sources, X-ray mirror optics, Atlas CCD detector, and low-temperature Cryojet device. The data were processed with the CrysAlis Pro package of programs (Agilent Technologies, 2011), followed by an empirical multi-scan correction using the SCALE3 ABSPACK routine. Structures were solved using the shelxs program and refined with shelxl³¹ in combination with the Olex2 crystallographic package.³² In most cases, hydrogen atoms were localized in difference syntheses of electron density but were refined using appropriate geometric restrictions of the corresponding bond lengths and bond angles within a riding/rotating model. X-ray crystallographic parameters are provided in Table 1 and experimental details are available in the corresponding CIFs.

Table 1. Summary of X-ray crystallographic data collection and structure refinement.

	NiFe ^{OAc} ·4 acetone	NiCo ^{OAc}	NiNi ^{OAc}	NiZn ^{OAc}	CoCo ^{OAc}	NiZn ^{OH} ·DCE	NiNi ^{OMe} ·M eOH
Empirical formula	C ₅₉ H ₈₉ FeN ₃ NiO ₁₁	C ₄₉ H ₆₉ CoN ₃ NiO ₇	C ₄₉ H ₆₉ N ₃ Ni ₂ O ₇	C ₄₉ H ₆₉ N ₃ Ni O ₇ Zn	C ₄₉ H ₆₉ Co ₂ N ₃ O ₇	C ₄₇ H ₆₃ N ₃ Ni ₂ O ₄ Cl ₂ Zn	C ₄₉ H ₇₃ N ₃ Ni ₂ O ₇
Formula weight	1130.89	929.71	929.49	936.15	929.93	928.98	933.52
Crystal system	monoclinic	monoclinic	monoclinic	monoclinic	monoclinic	monoclinic	monoclinic
Space group	<i>P</i> 2 ₁	<i>P</i> 2 ₁ / <i>n</i>	<i>P</i> 2 ₁ / <i>n</i>	<i>P</i> 2 ₁ / <i>n</i>	<i>P</i> 2 ₁ / <i>n</i>	<i>P</i> 2 ₁ / <i>c</i>	<i>P</i> 2 ₁ / <i>c</i>
<i>a</i> (Å)	10.3503(2)	10.21448(8)	10.1841(1)	10.2153(1)	10.2249(2)	14.4458(3)	20.8266(6)
<i>b</i> (Å)	20.2208(3)	20.4809(2)	20.5261(3)	20.4672(3)	20.6272(3)	19.0800(2)	13.0162(3)
<i>c</i> (Å)	15.6385(3)	22.7461(3)	22.8062(4)	22.7709(3)	22.7256(4)	17.1363(2)	18.9697(4)
α (°)	90	90	90	90	90	90	90
β (°)	107.257(2)	97.7635(9)	98.208(1)	97.818(1)	97.741(2)	106.356(2)	110.255(3)
γ (°)	90	90	90	90	90	90	90
<i>V</i> (Å ³)	3125.7(1)	4714.90(8)	4718.6(1)	4716.7(1)	4749.0(1)	4532.0(1)	4824.4(2)
<i>Z</i>	2	4	4	4	4	4	4
<i>D</i> _{calc} (g/cm ³)	1.202	1.310	1.308	1.318	1.301	1.362	1.285

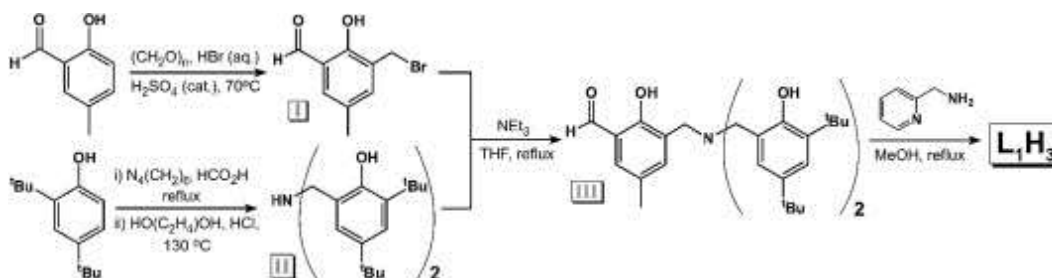
	NiFe ^{OAc} ·4 acetone	NiCo ^{OAc}	NiNi ^{OAc}	NiZn ^{OAc}	CoCo ^{OAc}	NiZn ^{OH} ·DCE	NiNi ^{OMe} ·M eOH
λ (Å)	0.7107	1.5418	0.7107	1.5418	0.7107	1.5418	1.5418
μ (mm ⁻¹)	0.589	3.67	0.851	1.539	0.751	2.606	1.378
θ -Range (°)	5.6–59.0	7.8–147.2	5.7–58.9	5.8–147.8	5.6–59.0	7.1–147.6	8.2–147.2
Reflections collected	36415	45296	40517	45332	38008	43809	45182
Independent reflections (R_{int})	14 441 (0.0338)	9423 (0.0284)	11 527 (0.0312)	9435 (0.0312)	11 671 (0.0289)	9000 (0.0357)	9558 (0.0416)
Data/restraints/parameters	14441/7/71 4	9423/0/57 4	11527/0/5 74	9435/0/57 4	11671/0/5 74	9000/5/559	9558/0/57 9
Goodness-of-fit (GOF) on F^2	1.042	1.041	1.067	1.023	1.033	1.031	1.043
R_1/wR_2 ($I > 2\sigma(I)$) ^a	0.0359/0.0768	0.0389/0.1097	0.0383/0.0880	0.0339/0.0924	0.0365/0.0878	0.0324/0.0847	0.0413/0.1137
R_1/wR_2 (all data) ^a	0.0422/0.0813	0.0430/0.1132	0.0485/0.0936	0.0392/0.0965	0.0475/0.0946	0.0375/0.0888	0.0482/0.1212

^a $R_1 = \sum ||F_o| - |F_c|| / \sum |F_o|$; $wR_2 = [\sum w(F_o^2 - F_c^2)^2 / \sum w(F_o^2)^2]^{1/2}$.

3. Results and discussion

3.1. Ligand and complex syntheses

The novel **L₁H₃** ligand was prepared in four steps via the route shown in Scheme 3. As demonstrated by Belostotskaya et al. the Duff-like reaction of 2,4-di-*tert*-butylphenol with hexamethylenetetramine in HCO₂H generates a benzoxazine intermediate that is converted to bis(3,5-di-*tert*-butyl-2-hydroxybenzyl)amine (**II**) in ethylene glycol and HCl. Bromomethylation of 5-methylsalicylaldehyde provided compound **I**, which participated in a substitution reaction with **II** under basic conditions to generate **III** in 53% yield. In the final step, the Schiff base and pyridyl donors of **L₁H₃** were incorporated by condensation of 2-picolylamine with the aldehyde moiety of **III**.



Scheme 3.

The homo- and heterobimetallic complexes **NiM^BOAc** (Scheme 2) were prepared by mixing equimolar amounts of **L₁H₃**, Ni(OAc)₂·4H₂O, and the appropriate M(OAc)₂ salt in MeOH (M^B = Fe, Co, Ni, or Zn).

Three equivalents of base (NaOMe) were required to deprotonate the phenolic groups of **L₁H₃**. The resulting complexes are soluble in CH₂Cl₂ and most polar aprotic solvents, but only sparingly soluble in MeOH. High-quality crystals were generally obtained from solvent mixtures involving MeOH and either CH₂Cl₂ or MeCN; the single exception was complex **NiFe^{OAc}**, which was crystallized from a 1:1 combination of acetone and MeCN.

Similar reaction conditions were used to generate the μ -OH complex, **NiZn^{OH}**, with three crucial differences: (i) the M^{II} ions were added as perchlorate salts, (ii) triethylamine (NEt₃) was used to deprotonate **L₁H₃**, and (iii) a single equivalent of (NEt₄)OH was added to supply the bridging ligand and induce precipitation. X-ray quality crystals of **NiZn^{OH}** were obtained by vapor diffusion of pentane into a concentrated DCE solution. The same approach was used in our attempts to prepare the corresponding dinickel(II) complex (*i.e.*, **NiNi^{OH}**), yet we were not able to grow suitable crystals from mixtures of DCE (or DCM) and pentane. X-ray quality crystals were obtained, however, from a mixture of MeCN and MeOH. The resulting structure (*vide infra*) revealed that the Ni^{II} centers are bridged by a solvent-derived methoxide ligand instead of the intended hydroxide group, giving rise to complex **NiNi^{OMe}**. This result indicates that the μ -OH ligand of **NiM_B^{OH}** is readily exchanged with ⁻OCH₃ in methanolic solution.

3.2. Crystallographic studies

Solid-state structures of the homo- and heterobimetallic complexes were collected using X-ray diffraction. Details concerning the crystallographic experiments and structure refinements are provided in Table 1. Complexes **NiCo^{OAc}**, **NiNi^{OAc}**, and **NiZn^{OAc}** yield quasi-isomorphous crystals in the monoclinic *P2₁/n* space group, whereas complex **NiFe^{OAc}** crystallizes in the non-centrosymmetric *P2₁* group. The structure of **NiZn^{OAc}**, shown in Fig. 1, is representative of the entire series. In each case, the trianionic **L₁³⁻** ligand supports a bimetallic core in which the metal centers are bridged by two donors: the central phenolate of **L₁³⁻** (O1) and a μ -1,1-acetate group (O4). The complexes are neutral overall due to the presence of the acetate ligand. As intended, the Ni^{II} center occupies the "tetragonal" position

(site **A**) defined by the Schiff-base (N2) and pyridyl (N3) donors in addition to the two bridging groups. Two solvent-derived ligands, either MeOH or H₂O, bind to Ni in a *trans* orientation. The M_B^{II} ion is located in the "tripodal" five-coordinate position (site **B**) attached to the amino donor (N1) and two terminal phenolates (O2 and O3).

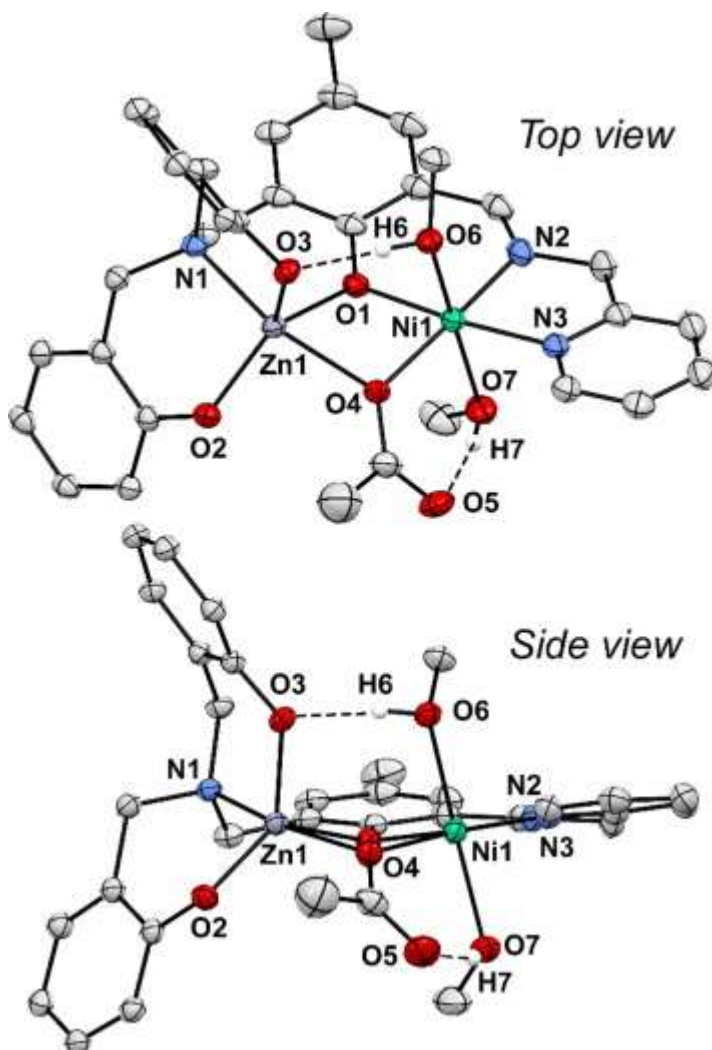


Fig. 1. Thermal ellipsoid plots (50% probability) derived from the X-ray structure of **NiZn**^{OAc}. Most hydrogen atoms and the *tert*-butyl substituents of the terminal phenolate donors have been removed for clarity.

Metal ion assignments were established by comparing *R*-factors and thermal parameters for the four possible configurations (two homobimetallic and two heterobimetallic). For complexes **NiFe**^{OAc} and **NiZn**^{OAc}, the experimental data strongly support the metal ion identities and positions indicated in Scheme 2; however, in the case of

NiCo^{OAc}, replacement of Co for Ni (or *vice versa*) causes little change in *R*-factor. We therefore synthesized the analogous dicobalt(II) complex, **CoCo^{OAc}**. Table 2 provides a quantitative comparison of bond distances and angles in the **NiNi^{OAc}**, **CoCo^{OAc}**, and **NiCo^{OAc}** structures. The three complexes have identical ligand sets and quasi-isomorphous unit cells; thus, any structural differences must be due to the presence of different metal ions in the **A** and **B** sites. The **B**-site metric parameters in the **CoCo^{OAc}** structure are nearly identical to those observed for **NiCo^{OAc}**, with root-mean-square (rms) deviations of merely 0.007 Å and 0.36° for metal–ligand bond distances and angles, respectively. In contrast, the **B**-sites in the **NiNi^{OAc}** and **NiCo^{OAc}** structures are significantly different (Table 2); in particular, the Ni2–N1 and Ni2–O4 distances are shorter in **NiNi^{OAc}** by ~0.06 Å, and the O1–M_B–O2 and O1–M_B–O3 angles shift by ~5°. Thus, it is clear that the **B**-site in **NiCo^{OAc}** is occupied by Co^{II}. For site **A**, the **NiCo^{OAc}** structure more closely matches **NiNi^{OAc}** than **CoCo^{OAc}** with respect to both bond lengths and angles (Table 2). We are confident, therefore, that the **NiCo^{OAc}** structure corresponds to a heterobimetallic complex with Ni^{II} in site **A** and Co^{II} in site **B**.

Table 2. Root-mean-square Deviations in Metal–Ligand Bond Distances (Å) and Angles (deg) for the A- and B-Sites within the **NiCo^{OAc}**, **CoCo^{OAc}**, and **NiNi^{OAc}** Structures.

		rms deviation from NiCo ^{OAc} structure	
		Site A	Site B
NiNi^{OAc}	bond distances (Å)	0.0140	0.0400
	bond angles (°)	1.14	2.54
CoCo^{OAc}	bond distances (Å)	0.0349	0.0066
	bond angles (°)	1.58	0.36

As shown in Table 3, metric parameters for structures in the **NiM_B^{OAc}** series exhibit little variation across the series. The presence of two monoatomic bridges results in short Ni_A···M_B distances of 3.12 ± 0.02 Å and average bridge angles (Ni–O–M^B) of 97°. The Ni···M_B distance is also reduced by the “puckering” of the [Ni–O(1/4)–M_B] diamond core, which deviates from planarity by nearly 19°. Each axial solvent ligand serves as an intramolecular hydrogen bond (H-bond) donor: one to the terminal phenolate group (O3), the other to the non-coordinating carbonyl moiety (O5) of acetate (Fig. 1). These interactions are facilitated by the aforementioned puckering of the

central core, which tilts the phenolate acceptor (O3) towards the H6–O6 donor of the proximal MeOH (or H₂O).

Table 3. Selected bond distances (Å) and bond angles (°) for **NiM_B^{OAc}** complexes (M_B = Fe, Co, Ni, Zn) and **NiNi^{OMe}** measured with X-ray diffraction.

	NiFe^{OAc}	NiCo^{OAc}	NiNi^{OAc}	NiZn^{OAc}	NiNi^{OMe}
<i>Bond distances</i>					
Ni(1)···M _B (1)	3.1165(4)	3.0960(5)	3.1210(3)	3.1329(4)	3.0744(4)
Ni(1)–N(2)	1.976(2)	1.981(2)	1.979(2)	1.976(2)	2.014(2)
Ni(1)–N(3)	2.072(2)	2.058(2)	2.053(2)	2.055(2)	2.085(2)
Ni(1)–O(1)	2.030(2)	2.032(1)	2.007(1)	2.025(1)	2.030(1)
Ni(1)–O(4)	2.042(2)	2.031(2)	2.047(1)	2.037(1)	1.977(1)
Ni(1)–O(6)	2.117(2)	2.116(2)	2.100(1)	2.107(1)	2.124(2)
Ni(1)–O(7)	2.119(2)	2.129(2)	2.134(2)	2.130(1)	2.128(1)
M _B (1)–N(1)	2.154(2)	2.094(2)	2.035(2)	2.095(1)	2.072(2)
M _B (1)–O(1)	2.116(2)	2.054(2)	2.070(1)	2.108(1)	2.059(1)
M _B (1)–O(2)	1.943(2)	1.940(1)	1.945(1)	1.933(1)	2.001(1)
M _B (1)–O(3)	1.983(2)	1.950(1)	1.959(1)	1.959(1)	1.999(1)
M _B (1)–O(4)	2.196(2)	2.199(1)	2.134(1)	2.174(1)	1.980(1)
<i>Bond-angles</i>					
Ni(1)–O(1)–M _B (1)	97.46(6)	98.53(6)	99.90(6)	98.57(5)	97.50(6)
Ni(1)–O(4)–M _B (1)	94.62(6)	94.02(6)	96.55(6)	96.07(5)	101.97(6)
O(1)–M _B (1)–O(2)	126.06(6)	129.00(6)	134.74(6)	129.11(5)	104.14(6)
O(1)–M _B (1)–O(3)	109.43(6)	110.52(6)	105.88(6)	108.73(5)	136.31(6)
O(1)–M _B (1)–O(4)	78.36(6)	78.48(5)	77.38(5)	77.02(5)	77.76(6)
O(1)–M _B (1)–N(1)	88.03(6)	90.34(6)	90.05(6)	89.06(5)	89.21(6)
O(2)–M _B (1)–O(3)	124.44(7)	119.85(6)	118.29(6)	121.23(5)	119.26(6)
O(2)–M _B (1)–O(4)	97.42(6)	95.17(5)	95.03(5)	95.33(5)	92.65(6)
O(2)–M _B (1)–N(1)	93.72(6)	95.15(6)	96.63(6)	96.83(5)	92.66(6)
O(3)–M _B (1)–O(4)	90.50(6)	87.96(6)	86.73(5)	87.31(5)	94.56(6)
O(3)–M _B (1)–N(1)	90.38(6)	92.12(6)	93.09(6)	93.22(5)	93.39(6)
O(4)–M _B (1)–N(1)	165.84(6)	168.05(6)	166.84(6)	165.43(5)	166.78(6)
τ-value ^a	0.66	0.65	0.54	0.61	0.51

^aFor a definition of the τ-value, see Ref.²⁶ Five-coordinate complexes with ideal square-pyramidal geometries have τ-values of 0.0, and those with ideal trigonal-bipyramidal geometries have values of 1.0.

In the **NiM_B^{OAc}** series, the Ni_A^{II} center exists in a distorted octahedral environment with *trans* angles of 174 ± 3° and *cis* angles ranging between 82° and 98°. The average nickel-ligand bond distance is 2.03 Å in the equatorial plane and 2.12 Å in the axial direction, consistent with the presence of a high-spin (*S* = 1) center. This conclusion is corroborated by the solid-state magnetic moment (μ_{eff}) of 2.69 μ_{B} measured for **NiZn^{OAc}**. The coordination geometries of the M_B centers are best described as trigonal-bipyramidal, as indicated by τ-

values greater than 0.50 ($\tau = 0$ for an ideal square-pyramid and 1 for an ideal trigonal bipyramid; Table 3).³³ The amino (N1) and acetate (O4) donors occupy the axial positions, while the phenolate donors (O1–O3) constitute the equatorial plane. For each complex, the M_B –L distances display considerable variability, ranging from 1.96(3) Å for the terminal phenolates to 2.17(4) Å for the axial M_B –O4 bond. The average M_B –L distance of ~ 2.05 Å, however, suggests that each M_B^{II} ion in the **NiM_B^{OAc}** series is high-spin. Indeed, the magnetic moment of 4.51 μ_B measured for solid **NiCo^{OAc}** is close to the spin-only value of 4.80 μ_B expected for a molecule with uncoupled $S = 1$ and $S = 3/2$ centers.

The X-ray structure of **NiZn^{OH}**, shown in Fig. 2, reveals a heterobimetallic [Ni(μ -OH)Zn] core supported by the **L₁³⁻** chelate. The μ -OH ligand forms an intramolecular H-bond with the O3 atom of a terminal phenolate donor. While the ZnNO₄ units in **NiZn^{OH}** and **NiZn^{OAc}** display similar metric parameters, the geometries of the Ni_A^{II} sites are quite different in the two structures. Since crystals of **NiZn^{OH}** were obtained from DCE/pentane, this structure lacks the solvent-derived ligands found in the **NiM_B^{OAc}** series. The Ni_A center of **NiZn^{OH}** adopts a four-coordinate geometry with Ni_A–O/N bond lengths of 1.85 ± 0.02 Å – approximately 0.17 Å shorter than the corresponding distances in the **NiZn^{OAc}** structure. These parameters suggest that the Ni_A^{II} center in **NiZn^{OH}** is low-spin ($S = 0$), consistent with its square-planar coordination environment. However, the magnetic moment of **NiZn^{OH}** powder is 1.43 μ_B at room temperature, nearly half-way between the spin-only limits of 0.0 ($S = 0$) and 2.83 μ_B ($S = 1$). Thus, it appears that a mixture of high- and low-spin Ni_A^{II} centers exist in the solid state. Regardless, in the **NiZn^{OH}** structure, the short Ni_A–O(1/4) distances bring the two metal centers closer together, resulting in a Ni_A⋯Zn_B distance of slightly less than 3.0 Å.

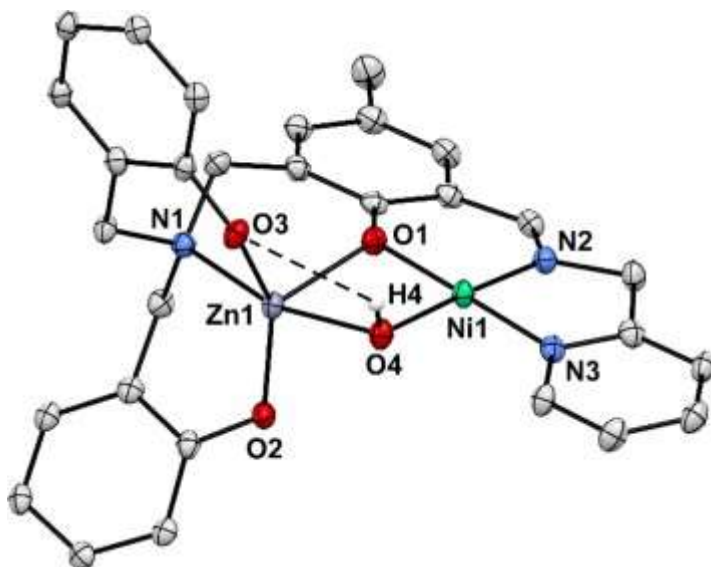


Fig. 2. Thermal ellipsoid plot (50% probability) derived from the X-ray structure of **NiZn^{OH}.DCE**. The non-coordinating DCE molecule, most hydrogen atoms, and the *tert*-butyl substituents of the terminal phenolate donors have been removed for clarity. Selected bond lengths (Å): Ni1...Zn1 2.9967(4), Ni1–O1 1.844(1), Ni–O4 1.859(1), Ni1–N2 1.841(2), Ni1–N3 1.870(2), Zn1–O1 2.127(1), Zn1–O2 1.950(1), Zn1–O3 1.964(1), Zn1–O4 2.054(1), Zn1–N1 2.138(1).

As noted above, our attempts to isolate the dinickel(II) analog of **NiZn^{OH}** were unsuccessful; however, X-ray quality crystals of **NiNi^{OMe}** can be grown by dissolving the putative **NiNi^{OH}** complex in a mixture of MeOH and MeCN. In the resulting structure, the second bridging position is occupied by methoxide (Scheme 2), but otherwise the geometry of **NiNi^{OMe}** is quite similar to that of **NiNi^{OAc}** (Fig. S1). In both cases, the binding of solvent-derived MeOH ligands gives rise to a six-coordinate, high-spin Ni_A^{II} center. A comparison of metric parameters reveals only minor differences between the two structures, although the Ni–OMe bond distances are noticeably shorter than the Ni–OAc distances (Table 3). Interestingly, whereas the **NiNi^{OAc}** structure features two intramolecular H-bonds, the replacement of acetate with methoxide forces one of the MeOH ligands to form an intermolecular H-bond with an outersphere MeOH molecule. This solvate, in turn, serves as a H-bond *donor* to the phenolate moiety of a second **NiNi^{OMe}** complex (Fig. S1).

3.3. Magnetic, Spectroscopic, and Electrochemical Properties in Solution

The magnetic moments of the **NiM_B^X** complexes in CHCl₃ solutions were determined using the Evans NMR method. The **NiZn^X** complexes exhibit μ_{eff} values of 2.67 (X = OAc) and 2.53 μ_{B} (X = OH), characteristic of $S = 1$ complexes. Thus, in contrast to its solid-state structure, the Ni^{II} center in **NiZn^{OH}** is unambiguously high-spin in solution, even in a non-coordinating solvent like CHCl₃. For complexes with two paramagnetic centers, the following values were measured: $\mu_{\text{eff}} = 3.82$ (**NiNi^{OAc}**), 3.77 (**NiNi^{OMe}**), 4.72 (**NiCo^{OAc}**), and 5.02 μ_{B} (**NiFe^{OAc}**). These experimental magnetic moments are slightly lower than the theoretical spin-only values expected for uncoupled paramagnets, indicating the presence of weak magnetic interactions between the metal centers.

UV-Vis absorption spectra of the reported **NiM_B^X** complexes were measured in DMF at room temperature; select data are shown in Fig. 3. Typical for complexes with high-spin Ni^{II} centers, the **NiZn^{OAc}** spectrum displays two bands in the visible region at 870 and 575 nm ($\epsilon = 8 \text{ M}^{-1} \text{ cm}^{-1}$) arising from the ${}^3\text{A}_{2\text{g}} \rightarrow {}^3\text{T}_{2\text{g}}$ and ${}^3\text{A}_{2\text{g}} \rightarrow {}^3\text{T}_{1\text{g}}(\text{F})$ transitions, respectively.³⁴ In addition, the spin-forbidden ${}^3\text{A}_{2\text{g}} \rightarrow {}^1\text{E}_{\text{g}}$ transition is evident at 750 nm. Complex **NiZn^{OH}** exhibits ligand-field transitions at similar energies, although the higher-energy band is obscured by features attributed to $\mu\text{-OH} \rightarrow \text{Ni}^{\text{II}}$ charge transfer (CT) transitions. Analysis of transition energies in the **NiZn^{OAc}** spectrum yields a ligand-field splitting (Δ_{o}) of 11500 cm^{-1} and Racah parameters of $B = 730 \text{ cm}^{-1}$ and $C = 3870 \text{ cm}^{-1}$ (the free ion B -value is 1030 cm^{-1}). These parameters are characteristic of six-coordinate Ni^{II} ions with partial pyridyl coordination.³⁴ In the **NiNi^{OAc}** spectrum, an "extra" ligand-field band arising from the second Ni^{II} center is apparent at 740 nm (Fig. 3(a)).

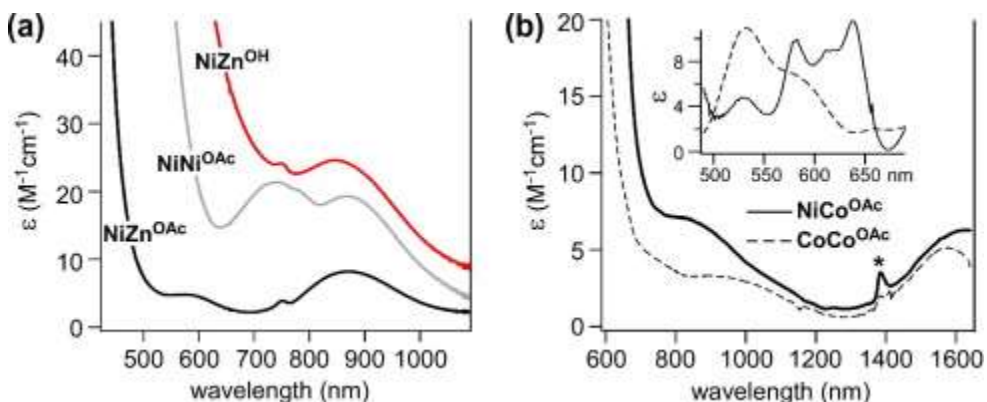


Fig. 3. Electronic absorption spectra of select $M_A M_B^X$ complexes measured at room temperature in DMF. The baselines of the $NiNi^{OAc}$ and $NiZn^{OH}$ spectra were shifted upward slightly to enhance clarity. The modified spectra shown in the inset of (b) were obtained *via* electronic subtraction of the broad absorption feature that trails into the visible region.

As shown in Fig. 3(b), both $NiCo^{OAc}$ and $CoCo^{OAc}$ exhibit two bands in the near infrared (NIR) region with $\lambda_{max} = \sim 1600$ and 1050 nm. As the $NiZn^X$ spectra are featureless in this region, these bands must arise from the Co^{II} center in the five-coordinate **B**-site. In addition, multiple Co^{II} -derived features appear as shoulders in the 500–650 nm region of the $NiCo^{OAc}$ and $CoCo^{OAc}$ spectra. These peaks are clearly evident in the inset of Fig. 3(b), where the broad absorption manifold that trails into the visible region has been removed (electronically) to provide a level baseline.¹ In order to assign these features, we have built upon the ligand-field approach developed by Ciampolini et al. in their seminal study of M^{II} ions in trigonal bipyramidal complexes.³⁵ Assuming approximate D_{3h} geometry, the 3d orbitals split into three levels: $E''(d_{xz}, d_{yz})$, $E'(d_{xy}, d_{x^2-y^2})$ and $A_1'(d_{z^2})$, listed in order of increasing energy. The conversion from O_h to pseudo- D_{3h} symmetry causes the T_{1g} and T_{2g} states to split into two components, as shown in Fig. 4. The ground state term symbol for high-spin d^7 ions is $^4A_2'$. Using this scheme, the band near 1600 nm (6250 cm^{-1}) can be assigned to the $^4A_2' \rightarrow ^4E''(F)$ transition that, in the strong field limit, corresponds to promotion of an $E''(d_{xz}, d_{yz})$ electron to the $E'(d_{xy}, d_{x^2-y^2})$ orbitals. The band at 1050 nm then arises from the $^4A_2' \rightarrow ^4E'(F)$ transition, and the two peaks at 640 and 580 nm spectrum are assigned to $^4A_2' \rightarrow ^4A_2'(P)$ and $^4A_2' \rightarrow ^4E''(P)$ transitions, respectively (these features appear in both spectra at roughly the same wavelengths). The weak peak at 610 nm in the $NiCo^{OAc}$ spectrum is tentatively assigned to the spin-forbidden

${}^4A_2' \rightarrow {}^2A_1'(G)$ transition, which gains intensity from the nearby spin-allowed transitions.

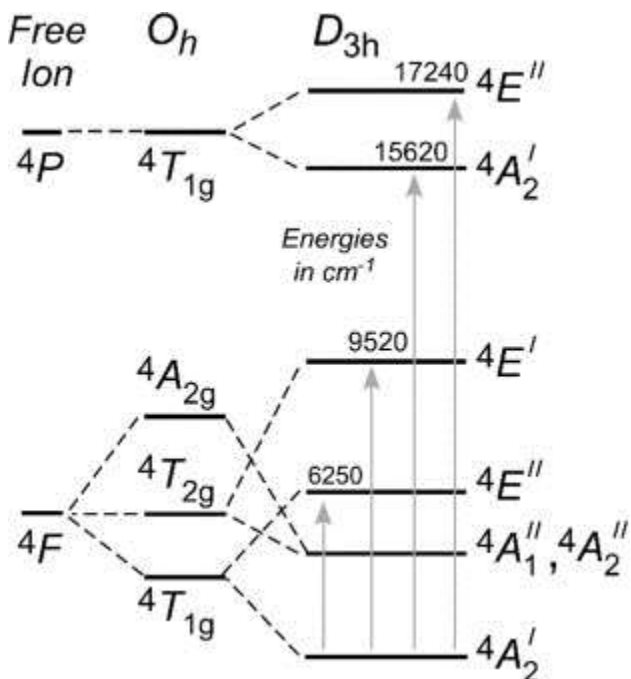


Fig. 4. Energy level diagram indicating the ligand-field states for a high-spin d^7 ion in three coordination environments: free ion, octahedral (O_h), and trigonal-bipyramidal (D_{3h}). The experimentally-determined transition energies for the Co^{II} ion in NiCo^{OAc} are provided in wavenumbers (cm^{-1}). Partially adapted from reference 27. Not to scale.

Analysis of the CoCo^{OAc} spectrum is more complex due to the presence of a second Co^{II} center in the **A**-site. Based on spectra reported for six-coordinate high-spin Co^{II} complexes,³⁴ the prominent band at 530 nm ($18\,870\text{ cm}^{-1}$) is assigned to the ${}^4T_{1g}(\text{F}) \rightarrow {}^4T_{1g}(\text{P})$ transition, while the corresponding ${}^4T_{1g}(\text{F}) \rightarrow {}^4T_{2g}(\text{F})$ transition (generally quite weak) is likely part of the broad absorption manifold centered at 1000 nm (Fig. 3(b)). Interestingly, the NiCo^{OAc} spectrum also exhibits a band at 530 nm, although its intensity is much lower. This result suggests that our NiCo^{OAc} sample is contaminated with a small amount of CoCo^{OAc} – a possibility previously considered in our analysis of the XRD data (*vide supra*).

The electrochemical properties of representative $\text{M}_A\text{M}_B^{\text{OAc}}$ complexes were examined by voltammetric methods in DMF solutions with 0.1 M $(\text{NBu}_4)\text{PF}_6$ as the supporting electrolyte and scan rates of 100 mV/s. As shown in Fig. 5, the cyclic voltammogram (CV) of

NiZn^{OA} displays a quasi-reversible redox couple at -1.17 V ($\Delta E = 0.20$ V) that corresponds to one-electron reduction of the Ni_A^{II} center (all potentials are relative to SCE). The CV's of **NiNi^{OA}** and **NiCo^{OA}** also feature a cathodic wave at -1.17 V due to the Ni ion in the **A**-site, but a second peak from the redox-active M_B^{II} ion is also apparent at more negative potentials (-1.36 V for **NiNi^{OA}** and 1.45 V for **NiCo^{OA}**). These redox events are very evident in the corresponding square-wave voltammograms (SWVs), represented by the dotted lines in Fig. 5. The **NiNi^{OA}** data indicate that the $\text{Ni}^{2+/+}$ potential is ~ 0.20 V lower in the **B**-site than the **A**-site, on account of the two terminal phenolate donors in the former. Interestingly, the CV and SWV data for **CoCo^{OA}** exhibit a single cathodic feature at -1.44 V with approximately twice the intensity of those observed for **NiCo^{OA}**, suggesting that the two Co^{II} ions are reduced at nearly identical potentials. The **M_AM_B^{OA}** complexes are also susceptible to irreversible oxidations, as indicated by the electrochemical data in Fig. S2; however, these anodic features are less well-defined than their cathodic counterparts, especially in the case of **NiZn^{OA}**. Complexes containing a redox-active M_B ion—**NiNi^{OA}**, **NiCo^{OA}**, and **CoCo^{OA}**—each display an irreversible peak near 0.30 V that is assigned to one-electron oxidation of the M_B^{II} center. An additional irreversible feature is evident near 0.75 V that, based on literature precedents,^{36;37;38} likely arises from oxidation of one (or more) of the phenolate groups in **L₁³⁻** to give a phenoxyl radical species.

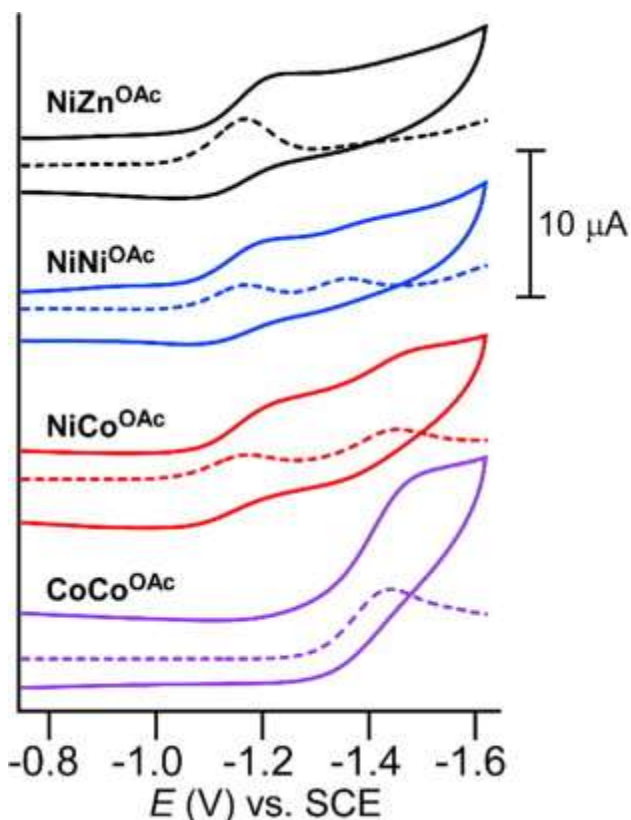


Fig. 5. Cyclic voltammograms (solid lines) of **NiZn^{OAc}**, **NiNi^{OAc}**, **NiCo^{OAc}**, and **CoCo^{OAc}** collected in DMF with 0.1 M (NBu₄)PF₆ as the supporting electrolyte and scan rates of 100 mV/s. The corresponding square-wave voltammograms are indicated by the dashed lines. In all cases the voltammogram was initiated by the cathodic sweep. The solution concentrations were 2.0 mM.

4. Conclusions

In this manuscript, we have described the synthesis and coordination chemistry of a new unsymmetric ligand (**L₁H₃**) designed to support heterobimetallic structures. The Schiff-base and pyridyl donors of the tetragonal **A**-site favor Ni^{II} binding, while the phenolate donors of the tripodal **B**-site are capable of coordinating various M^{II} ions (M = Fe, Co, Ni, Zn). In X-ray crystal structures of the resulting **M_AM_B^X** complexes, the two M^{II} centers are bridged by the central phenolate donor of **L₁³⁻** and an X anion, where X = μ -1,1-OAc, -OH, or -OCH₃. With the exception of the Ni_A^{II} center in the solid-state structure of **NiZn^{OH}**, the M^{II} ions in both coordination sites are high-spin, as determined by detailed analyses of structural parameters, UV-Vis-NIR absorption spectra, and magnetic susceptibility measurements. The Ni_A^{II} centers undergo one-electron reduction at

–1.17 V (*versus* SCE), while the Ni^B and Co^B ions are reduced at lower potentials.

As stated in the Introduction, our efforts were inspired by the active site of CODH, which utilizes a NiFe1 unit and a nearby [Fe₃S₄] cluster to reversibly reduce CO₂ to CO and H₂O. The bimetallic complexes described here reproduce several key features of the Ni-Fe1 fragment in CODH. Similar to enzymatic active site, the **NiM^B^X** complexes position a redox-active Ni^{II} center in close proximity to a second transition metal; indeed, the Ni^A···M^B distances of 3.03.1 Å observed in the **NiM^B^X** series are close to the average NiFe1 distance of ~2.8 Å found in CODH.⁸ It is our intention that the M^B ion will facilitate CO₂ activation by serving as a Lewis acid and (perhaps) a source of reducing equivalents; thus, the **B**-site contains three phenolate anions to depress the M^B redox potential. The Ni center in CODH has three “permanent” ligands: the thiolate of Cys526 and two sulfides from the [Fe₃S₄] cluster (Scheme 1). Likewise, the Ni^A centers are bound to only three **L₁**-derived donors, thereby providing three exchangeable coordination sites in a meridional arrangement. The presence of *cis*-labile sites is expected to be advantageous for CO₂ binding and activation, since studies of CODH suggest that the energetic barrier to C–O bond cleavage (typically the rate-determining step³⁹) is lowered if the resulting hydroxide is able to adopt a bridging position between two metal centers.^{9;10} Given these promising structural features, we are currently exploring the ability of the **NiM^B^X** series to serve as electrocatalysts for CO₂ reduction. We also plan to incorporate redox-active donors into the **L₁** framework; such moieties could serve as electron reservoirs in multi-electron processes, similar to the role of the [Fe₃S₄] cluster in the catalytic cycle of CODH.

Acknowledgements

This research is generously supported by Marquette University and the U.S. National Science Foundation (NSF) (CHE-1056845).

References

- ¹J.L. Boer, S.B. Mulrooney, R.P. Hausinger. *Arch. Biochem. Biophys.*, 544 (2014), p. 142

- ²S.W. Ragsdale, E. Pierce. *Biochim. Biophys. Acta, Proteins Proteomics*, 1784 (2008), p. 1873
- ³A. Volbeda, M.-H. Charon, C. Piras, E.C. Hatchikian, M. Frey, J.C. Fontecilla-Camps. *Nature*, 373 (1995), p. 580
- ⁴A. Volbeda, J.C. Fontecilla-Camps. *Coord. Chem. Rev.*, 249 (2005), p. 1609
- ⁵M. Bruschi, G. Zampella, P. Fantucci, G.L. De. *Coord. Chem. Rev.*, 249 (2005), p. 1620
- ⁶H. Ogata, W. Lubitz, Y. Higuchi. *Dalton Trans.* (2009), p. 7577
- ⁷C.L. Drennan, T.I. Doukov, S.W. Ragsdale. *J. Biol. Inorg. Chem.*, 9 (2004), p. 511
- ⁸Y. Kung, C.L. Drennan. *Curr. Opin. Chem. Biol.*, 15 (2011), p. 276
- ⁹A. Volbeda, J.C. Fontecilla-Camps. *Dalton Trans.* (2005), p. 3443
- ¹⁰P. Amara, J.-M. Mouesca, A. Volbeda, J.C. Fontecilla-Camps. *Inorg. Chem.*, 50 (2011), p. 1868
- ¹¹J.-H. Jeoung, H. Dobbek. *Science*, 318 (2007), p. 1461
- ¹²J.-H. Jeoung, H. Dobbek. *J. Biol. Inorg. Chem.*, 17 (2012), p. 167
- ¹³D. Huang, R.H. Holm. *J. Am. Chem. Soc.*, 132 (2010), p. 4693
- ¹⁴X. Zhang, D. Huang, Y.-S. Chen, R.H. Holm. *Inorg. Chem.*, 51 (2012), p. 11017
- ¹⁵C. Uyeda, J.C. Peters. *Chem. Sci.*, 4 (2013), p. 157
- ¹⁶S. Hazra, S. Bhattacharya, M.K. Singh, L. Carrella, E. Rentschler, T. Weyhermueller, G. Rajaraman, S. Mohanta. *Inorg. Chem.*, 52 (2013), p. 12881
- ¹⁷H. Kon, T. Nagata. *Dalton Trans.*, 42 (2013), p. 5697
- ¹⁸M. Jarenmark, M. Haukka, S. Demeshko, F. Tuczec, L. Zuppiroli, F. Meyer, E. Nordlander. *Inorg. Chem.*, 50 (2011), p. 3866
- ¹⁹S. Yao, C. Herwig, Y. Xiong, A. Company, E. Bill, C. Limberg, M. Driess. *Angew. Chem., Int. Ed.*, 49 (2010), p. 7054
- ²⁰A. Roth, A. Buchholz, M. Rudolph, E. Schuetze, E. Kothe, W. Plass. *Chem.-Eur. J.*, 14 (2008), p. 1571
- ²¹K. Danjobara, Y. Mitsuka, Y. Miyasato, M. Ohba, H. Okawa. *Bull. Chem. Soc. Jpn.*, 76 (2003), p. 1769
- ²²S.K. Dutta, R. Werner, U. Floerke, S. Mohanta, K.K. Nanda, W. Haase, K. Nag. *Inorg. Chem.*, 35 (1996), p. 2292
- ²³T.R. Holman, C. Juarez-Garcia, M.P. Hendrich, L. Que Jr., E. Munck. *J. Am. Chem. Soc.*, 112 (1990), p. 7611
- ²⁴M. Jarenmark, H. Carlsson, E. Nordlander. *C.R. Chim.*, 10 (2007), p. 433
- ²⁵C. Belle, J.-L. Pierre. *Eur. J. Inorg. Chem.* (2003), p. 4137
- ²⁶L.J. Daumann, G. Schenk, D.L. Ollis, L.R. Gahan. *Dalton Trans.*, 43 (2014), p. 910
- ²⁷N.G. Connelly, W.E. Geiger. *Chem. Rev.*, 96 (1996), p. 877
- ²⁸Q. Wang, C. Wilson, A.J. Blake, S.R. Collinson, P.A. Tasker, M. Schroeder. *Tetrahedron Lett.*, 47 (2006), p. 8983

- ²⁹I.S. Belostotskaya, N.L. Komissarova, T.I. Prokof'eva, L.N. Kurkovskaya, V.B. Vol'eva. *Russ. J. Org. Chem.*, 41 (2005), p. 703
- ³⁰I.A. Koval, D. Pursche, A.F. Stassen, P. Gamez, B. Krebs, J. Reedijk. *Eur. J. Inorg. Chem.* (2003), p. 1669
- ³¹G.M. Sheldrick. *Acta Crystallogr., Sect. A*, 64 (2008), p. 112
- ³²O.V. Dolomanov, L.J. Bourhis, R.J. Gildea, J.A.K. Howard, H. Puschmann. *J. Appl. Crystallogr.*, 42 (2009), p. 339
- ³³A.W. Addison, T.N. Rao, J. Reedijk, J. Vanriijn, G.C. Verschoor. *J. Chem. Soc., Dalton Trans.* (1984), p. 1349
- ³⁴A.B.P. Lever. *Inorganic Electronic Spectroscopy*. Elsevier, Amsterdam (1968)
- ³⁵M. Ciampolini, N. Nardi, G.P. Speroni. *Coord. Chem. Rev.*, 1 (1966), p. 222
- ³⁶M.M. Allard, J.A. Sonk, M.J. Heeg, B.R. McGarvey, H.B. Schlegel, C.N. Verani. *Angew. Chem., Int. Ed.*, 51 (2012), p. 3178
- ³⁷M. Lanznaster, H.P. Hratchian, M.J. Heeg, L.M. Hryhorczuk, B.R. McGarvey, H.B. Schlegel, C.N. Verani. *Inorg. Chem.*, 45 (2006), p. 955
- ³⁸B. Adam, E. Bill, E. Bothe, B. Goerdts, G. Haselhorst, K. Hildenbrand, A. Sokolowski, S. Steenken, T. Weyhermüller, K. Wieghardt. *Chem. Eur. J.*, 3 (1997), p. 308
- ³⁹A.M. Appel, J.E. Bercaw, A.B. Bocarsly, H. Dobbek, D.L. DuBois, M. Dupuis, J.G. Ferry, E. Fujita, R. Hille, P.J.A. Kenis, C.A. Kerfeld, R.H. Morris, C.H.F. Peden, A.R. Portis, S.W. Ragsdale, T.B. Rauchfuss, J.N.H. Reek, L.C. Seefeldt, R.K. Thauer, G.L. Waldrop. *Chem. Rev.*, 113 (2013), p. 6621

¹The background feature was modeled as a simple Gaussian curve in order to avoid introducing spurious features into the experimental spectrum.

Appendix A. Supplementary material

checkCIF/PLATON report

You have not supplied any structure factors. As a result the full set of tests cannot be run.

THIS REPORT IS FOR GUIDANCE ONLY. IF USED AS PART OF A REVIEW PROCEDURE FOR PUBLICATION, IT SHOULD NOT REPLACE THE EXPERTISE OF AN EXPERIENCED CRYSTALLOGRAPHIC REFEREE.

No syntax errors found. CIF dictionary Interpreting this report

Datablock: NiFe-OAc

Bond precision:	C-C = 0.0034 A	Wavelength=0.71070	
Cell:	a=10.3503(2)	b=20.2208(3)	c=15.6385(3)
	alpha=90	beta=107.257(2)	gamma=90
Temperature:	100 K		
	Calculated	Reported	
Volume	3125.67(10)	3125.67(10)	
Space group	P 21	P 1 21 1	
Hall group	P 2yb	P 2yb	
Moiety formula	C47 H65 Fe N3 Ni O7, 4(C3 H6 O)	C47 H65 Fe N3 Ni O7, 4(C3 H6 O)	
Sum formula	C59 H89 Fe N3 Ni O11	C59 H89 Fe N3 Ni O11	
Mr	1130.87	1130.89	
Dx,g cm-3	1.202	1.202	
Z	2	2	
Mu (mm-1)	0.589	0.589	
F000	1212.0	1212.0	
F000'	1213.84		
h,k,lmax	14,28,21	14,27,21	
Nref	17400[8934]	14441	
Tmin,Tmax	0.768,0.839	0.786,0.890	
Tmin'	0.724		

Correction method= GAUSSIAN

Data completeness= 1.62/0.83 Theta(max)= 29.480

R(reflections)= 0.0359(13259) wR2(reflections)= 0.0813(14441)

S = 1.042 Npar= Npar = 714

The following ALERTS were generated. Each ALERT has the format

test-name_ALERT_alert-type_alert-level.

Click on the hyperlinks for more details of the test.

Alert level B

Crystal system given = monoclinic

PLAT201_ALERT_2_B Isotropic non-H Atoms in Main Residue(s) 3 Why ?

Alert level C

PLAT202_ALERT_3_C Isotropic non-H Atoms in Anion/Solvent 4
PLAT244_ALERT_4_C Low 'Solvent' Ueq as Compared to Neighbors of C4S Check
PLAT244_ALERT_4_C Low 'Solvent' Ueq as Compared to Neighbors of C7S Check
PLAT244_ALERT_4_C Low 'Solvent' Ueq as Compared to Neighbors of C10S Check

Alert level G

PLAT002_ALERT_2_G Number of Distance or Angle Restraints on AtSite 8 Note
PLAT005_ALERT_5_G No _iucr_refine_instructions_details in the CIF Please Do !
PLAT301_ALERT_3_G Main Residue Disorder Percentage = 5 Note
PLAT302_ALERT_4_G Anion/Solvent Disorder Percentage = 25 Note
PLAT710_ALERT_4_G Delete 1-2-3 or 2-3-4 Linear Torsion Angle ... # 25 Do !
O1 -Ni1 -N3 -C11 54.40 0.50 1.555 1.555 1.555 1.555
PLAT710_ALERT_4_G Delete 1-2-3 or 2-3-4 Linear Torsion Angle ... # 26 Do !
O1 -Ni1 -N3 -C15 -115.70 0.50 1.555 1.555 1.555 1.555
PLAT710_ALERT_4_G Delete 1-2-3 or 2-3-4 Linear Torsion Angle ... # 58 Do !
O4 -Ni1 -N2 -C9 -6.70 1.50 1.555 1.555 1.555 1.555
PLAT710_ALERT_4_G Delete 1-2-3 or 2-3-4 Linear Torsion Angle ... # 59 Do !
O4 -Ni1 -N2 -C10 174.00 1.30 1.555 1.555 1.555 1.555
PLAT710_ALERT_4_G Delete 1-2-3 or 2-3-4 Linear Torsion Angle ... # 99 Do !
N2 -Ni1 -O4 -FE1 16.90 1.40 1.555 1.555 1.555 1.555
PLAT710_ALERT_4_G Delete 1-2-3 or 2-3-4 Linear Torsion Angle ... # 100 Do !
N2 -Ni1 -O4 -C46 -135.60 1.30 1.555 1.555 1.555 1.555
PLAT710_ALERT_4_G Delete 1-2-3 or 2-3-4 Linear Torsion Angle ... # 105 Do !
N3 -Ni1 -O1 -FE1 108.90 0.50 1.555 1.555 1.555 1.555
PLAT710_ALERT_4_G Delete 1-2-3 or 2-3-4 Linear Torsion Angle ... # 106 Do !
N3 -Ni1 -O1 -C3 -40.60 0.50 1.555 1.555 1.555 1.555
PLAT720_ALERT_4_G Number of Unusual/Non-Standard Labels 24 Note
PLAT790_ALERT_4_G Centre of Gravity not Within Unit Cell: Resd. # 5 Note
C3 H6 O
PLAT860_ALERT_3_G Number of Least-Squares Restraints 7 Note

0 **ALERT level A** = Most likely a serious problem - resolve or explain
1 **ALERT level B** = A potentially serious problem, consider carefully
4 **ALERT level C** = Check. Ensure it is not caused by an omission or oversight
15 **ALERT level G** = General information/check it is not something unexpected

0 ALERT type 1 CIF construction/syntax error, inconsistent or missing data
2 ALERT type 2 Indicator that the structure model may be wrong or deficient
3 ALERT type 3 Indicator that the structure quality may be low
14 ALERT type 4 Improvement, methodology, query or suggestion
1 ALERT type 5 Informative message, check

Datablock: CoNi-OAc

Bond precision: C-C = 0.0032 A

Wavelength=1.54184

Cell: a=20.4809(2) b=22.7461(3) c=90
 alpha=97.7635(9) beta=90 gamma=
 Temperature: 100 K

	Calculated	Reported
Volume	4714.91(9)	4714.90(8)
Space group	P 21/n	P 1 21/n 1
Hall group	-P 2yn	-P 2yn
Moiety formula	C49 H69 Co N3 Ni O7	C49 H69 Co N3 Ni O7
Sum formula	C49 H69 Co N3 Ni O7	C49 H69 Co N3 Ni O7
Mr	929.69	929.71
Dx,g cm-3	1.310	1.310
Z	4	4
Mu (mm-1)	3.670	3.670
F000	1980.0	1980.0
F000'	1963.58	
h,k,lmax	12,25,28	12,25,28
Nref	9515	9423
Tmin,Tmax	0.432,0.691	0.482,0.785
Tmin'	0.249	

Correction method= GAUSSIAN

Data completeness= 0.990 Theta(max)= 73.580

R(reflections)= 0.0389(8638) wR2(reflections)= 0.1132(9423)

S = 1.041 Npar= Npar = 574

The following ALERTS were generated. Each ALERT has the format

test-name_ALERT_alert-type_alert-level.

Click on the hyperlinks for more details of the test.

Alert level C

PLAT413_ALERT_2_C Short Inter XH3 .. XHn H7C .. H43C .. 2.14 Ang.

Alert level G

PLAT005_ALERT_5_G No _iucr_refine_instructions_details in the CIF Please Do !
 PLAT142_ALERT_4_G su on b - Axis Small or Missing 0.00020 Ang.
 PLAT710_ALERT_4_G Delete 1-2-3 or 2-3-4 Linear Torsion Angle ... # 27 Do !
 O1 -NI1 -N3 -C11 -30.80 0.80 1.555 1.555 1.555 1.555
 PLAT710_ALERT_4_G Delete 1-2-3 or 2-3-4 Linear Torsion Angle ... # 28 Do !
 O1 -NI1 -N3 -C15 148.70 0.60 1.555 1.555 1.555 1.555
 PLAT710_ALERT_4_G Delete 1-2-3 or 2-3-4 Linear Torsion Angle ... # 64 Do !
 O4 -NI1 -N2 -C9 39.00 0.80 1.555 1.555 1.555 1.555
 PLAT710_ALERT_4_G Delete 1-2-3 or 2-3-4 Linear Torsion Angle ... # 65 Do !
 O4 -NI1 -N2 -C10 -130.10 0.60 1.555 1.555 1.555 1.555
 PLAT710_ALERT_4_G Delete 1-2-3 or 2-3-4 Linear Torsion Angle ... # 79 Do !
 O6 -NI1 -O7 -C49 144.80 0.50 1.555 1.555 1.555 1.555
 PLAT710_ALERT_4_G Delete 1-2-3 or 2-3-4 Linear Torsion Angle ... # 88 Do !

O7	-Ni1	-O6	-C48	154.10	0.50	1.555	1.555	1.555	1.555	
PLAT710_ALERT_4_G	Delete	1-2-3	or 2-3-4	Linear	Torsion	Angle ...	#			105 Do !
N2	-Ni1	-O4	-CO1	-58.10	0.70	1.555	1.555	1.555	1.555	
PLAT710_ALERT_4_G	Delete	1-2-3	or 2-3-4	Linear	Torsion	Angle ...	#			106 Do !
N2	-Ni1	-O4	-C46	92.20	0.70	1.555	1.555	1.555	1.555	
PLAT710_ALERT_4_G	Delete	1-2-3	or 2-3-4	Linear	Torsion	Angle ...	#			113 Do !
N3	-Ni1	-O1	-CO1	-139.90	0.70	1.555	1.555	1.555	1.555	
PLAT710_ALERT_4_G	Delete	1-2-3	or 2-3-4	Linear	Torsion	Angle ...	#			114 Do !
N3	-Ni1	-O1	-C1	13.40	0.80	1.555	1.555	1.555	1.555	

0 **ALERT level A** = Most likely a serious problem - resolve or explain
0 **ALERT level B** = A potentially serious problem, consider carefully
1 **ALERT level C** = Check. Ensure it is not caused by an omission or oversight
12 **ALERT level G** = General information/check it is not something unexpected

0 ALERT type 1 CIF construction/syntax error, inconsistent or missing data
1 ALERT type 2 Indicator that the structure model may be wrong or deficient
0 ALERT type 3 Indicator that the structure quality may be low
11 ALERT type 4 Improvement, methodology, query or suggestion
1 ALERT type 5 Informative message, check

Datablock: NiNi-OAc

Bond precision: C-C = 0.0030 A

Wavelength=0.71073

Cell: a=20.5261(3)
alpha=98.2084(13)

b=22.8062(4) c=90
beta=90 gamma=

Temperature: 100 K

	Calculated	Reported
Volume	4718.54(13)	4718.56(12)
Space group	P 21/n	P 1 21/n 1
Hall group	-P 2yn	-P 2yn
Moiety formula	C49 H69 N3 Ni2 O7	C49 H69 N3 Ni2 O7
Sum formula	C49 H69 N3 Ni2 O7	C49 H69 N3 Ni2 O7
Mr	929.45	929.49
Dx,g cm-3	1.308	1.308
Z	4	4
Mu (mm-1)	0.851	0.851
F000	1984.0	1984.0
F000'	1987.40	
h,k,lmax	14,28,31	13,26,30
Nref	13109	11527
Tmin,Tmax	0.752,0.898	0.802,0.903
Tmin'	0.699	

Correction method= GAUSSIAN

Data completeness= 0.879

Theta(max)= 29.470

R(reflections)= 0.0383(9851) wR2(reflections)= 0.0936(11527)

S = 1.067

Npar= Npar = 574

The following ALERTS were generated. Each ALERT has the format

test-name_ALERT_alert-type_alert-level.

Click on the hyperlinks for more details of the test.

● **Alert level C**

PLAT413_ALERT_2_C Short Inter XH3 .. XHn H7C .. H43C .. 2.13 Ang.

● **Alert level G**

PLAT005_ALERT_5_G No _iucr_refine_instructions_details in the CIF Please Do !
PLAT710_ALERT_4_G Delete 1-2-3 or 2-3-4 Linear Torsion Angle ... # 27 Do !
 O1 -NI1 -N3 -C11 -35.40 0.70 1.555 1.555 1.555 1.555
PLAT710_ALERT_4_G Delete 1-2-3 or 2-3-4 Linear Torsion Angle ... # 28 Do !
 O1 -NI1 -N3 -C15 143.20 0.60 1.555 1.555 1.555 1.555
PLAT710_ALERT_4_G Delete 1-2-3 or 2-3-4 Linear Torsion Angle ... # 64 Do !
 O4 -NI1 -N2 -C9 36.60 0.50 1.555 1.555 1.555 1.555
PLAT710_ALERT_4_G Delete 1-2-3 or 2-3-4 Linear Torsion Angle ... # 65 Do !
 O4 -NI1 -N2 -C10 -132.30 0.40 1.555 1.555 1.555 1.555
PLAT710_ALERT_4_G Delete 1-2-3 or 2-3-4 Linear Torsion Angle ... # 79 Do !
 O6 -NI1 -O7 -C49 143.80 0.40 1.555 1.555 1.555 1.555
PLAT710_ALERT_4_G Delete 1-2-3 or 2-3-4 Linear Torsion Angle ... # 88 Do !
 O7 -NI1 -O6 -C48 154.00 0.40 1.555 1.555 1.555 1.555
PLAT710_ALERT_4_G Delete 1-2-3 or 2-3-4 Linear Torsion Angle ... # 105 Do !
 N2 -NI1 -O4 -NI2 -56.40 0.40 1.555 1.555 1.555 1.555
PLAT710_ALERT_4_G Delete 1-2-3 or 2-3-4 Linear Torsion Angle ... # 106 Do !
 N2 -NI1 -O4 -C46 98.90 0.40 1.555 1.555 1.555 1.555
PLAT710_ALERT_4_G Delete 1-2-3 or 2-3-4 Linear Torsion Angle ... # 113 Do !
 N3 -NI1 -O1 -NI2 -137.70 0.60 1.555 1.555 1.555 1.555
PLAT710_ALERT_4_G Delete 1-2-3 or 2-3-4 Linear Torsion Angle ... # 114 Do !
 N3 -NI1 -O1 -C1 21.20 0.70 1.555 1.555 1.555 1.555
PLAT951_ALERT_5_G Reported and Calculated Kmax Values Differ by .. 2

0 **ALERT level A** = Most likely a serious problem - resolve or explain
0 **ALERT level B** = A potentially serious problem, consider carefully
1 **ALERT level C** = Check. Ensure it is not caused by an omission or oversight
12 **ALERT level G** = General information/check it is not something unexpected

0 ALERT type 1 CIF construction/syntax error, inconsistent or missing data
1 ALERT type 2 Indicator that the structure model may be wrong or deficient
0 ALERT type 3 Indicator that the structure quality may be low
10 ALERT type 4 Improvement, methodology, query or suggestion
2 ALERT type 5 Informative message, check

Datablock: NiZn-OAc

Bond precision: C-C = 0.0028 A

Wavelength=1.54180

Cell: a=20.4672(3) b=22.7709(3) c=90
 alpha=97.8176(12) beta=90 gamma=
 Temperature: 100 K

	Calculated	Reported
Volume	4716.66(11)	4716.66(11)
Space group	P 21/n	P 1 21/n 1
Hall group	-P 2yn	-P 2yn
Moiety formula	C49 H69 N3 Ni O7 Zn	C49 H69 N3 Ni O7 Zn
Sum formula	C49 H69 N3 Ni O7 Zn	C49 H69 N3 Ni O7 Zn
Mr	936.15	936.15
Dx,g cm-3	1.318	1.318
Z	4	4
Mu (mm-1)	1.539	1.539
F000	1992.0	1992.0
F000'	1978.74	
h,k,lmax	12,25,28	12,24,28
Nref	9565	9435
Tmin,Tmax	0.774,0.846	0.770,0.867
Tmin'	0.692	

Correction method= GAUSSIAN

Data completeness= 0.986 Theta(max)= 73.880


R(reflections)= 0.0339(8397) wR2(reflections)= 0.0965(9435)

S = 1.023 Npar= Npar = 574

The following ALERTS were generated. Each ALERT has the format


test-name_ALERT_alert-type_alert-level.

Click on the hyperlinks for more details of the test.


 **Alert level B**

Crystal system given = monoclinic

PLAT230_ALERT_2_B Hirshfeld Test Diff for C46 -- C47 .. 11.5 su

 **Alert level C**

PLAT220_ALERT_2_C Large Non-Solvent C Ueq(max)/Ueq(min) Range 3.1 Ratio

 **Alert level G**

PLAT005_ALERT_5_G No _iucr_refine_instructions_details in the CIF Please Do !
 PLAT710_ALERT_4_G Delete 1-2-3 or 2-3-4 Linear Torsion Angle ... # 34 Do !
 O1 -NI1 -N3 -C11 -29.80 0.70 1.555 1.555 1.555 1.555
 PLAT710_ALERT_4_G Delete 1-2-3 or 2-3-4 Linear Torsion Angle ... # 35 Do !
 O1 -NI1 -N3 -C15 149.70 0.60 1.555 1.555 1.555 1.555
 PLAT710_ALERT_4_G Delete 1-2-3 or 2-3-4 Linear Torsion Angle ... # 69 Do !
 O4 -NI1 -N2 -C9 39.60 0.60 1.555 1.555 1.555 1.555
 PLAT710_ALERT_4_G Delete 1-2-3 or 2-3-4 Linear Torsion Angle ... # 70 Do !

O4	-NI1 -N2	-C10	-130.40	0.50	1.555	1.555	1.555	1.555	
PLAT710_ALERT_4_G	Delete	1-2-3 or 2-3-4	Linear	Torsion Angle ... #					77 Do !
O6	-NI1 -O7	-C49	147.60	0.40	1.555	1.555	1.555	1.555	
PLAT710_ALERT_4_G	Delete	1-2-3 or 2-3-4	Linear	Torsion Angle ... #					86 Do !
O7	-NI1 -O6	-C48	152.10	0.40	1.555	1.555	1.555	1.555	
PLAT710_ALERT_4_G	Delete	1-2-3 or 2-3-4	Linear	Torsion Angle ... #					105 Do !
N2	-NI1 -O4	-ZN1	-59.00	0.50	1.555	1.555	1.555	1.555	
PLAT710_ALERT_4_G	Delete	1-2-3 or 2-3-4	Linear	Torsion Angle ... #					106 Do !
N2	-NI1 -O4	-C46	92.00	0.50	1.555	1.555	1.555	1.555	
PLAT710_ALERT_4_G	Delete	1-2-3 or 2-3-4	Linear	Torsion Angle ... #					113 Do !
N3	-NI1 -O1	-ZN1	-141.10	0.60	1.555	1.555	1.555	1.555	
PLAT710_ALERT_4_G	Delete	1-2-3 or 2-3-4	Linear	Torsion Angle ... #					114 Do !
N3	-NI1 -O1	-C3	11.40	0.70	1.555	1.555	1.555	1.555	

0 **ALERT level A** = Most likely a serious problem - resolve or explain
 1 **ALERT level B** = A potentially serious problem, consider carefully
 1 **ALERT level C** = Check. Ensure it is not caused by an omission or oversight
 11 **ALERT level G** = General information/check it is not something unexpected

0 ALERT type 1 CIF construction/syntax error, inconsistent or missing data
 2 ALERT type 2 Indicator that the structure model may be wrong or deficient
 0 ALERT type 3 Indicator that the structure quality may be low
 10 ALERT type 4 Improvement, methodology, query or suggestion
 1 ALERT type 5 Informative message, check

Datablock: CoCo-OAc

Bond precision:	C-C = 0.0027 A	Wavelength=0.71073	
Cell:	a=20.6272(3)	b=22.7256(4)	c=90
	alpha=97.7409(17)	beta=90	gamma=
Temperature:	100 K		
	Calculated	Reported	
Volume	4748.98(13)	4748.98(14)	
Space group	P 21/n	P 1 21/n 1	
Hall group	-P 2yn	-P 2yn	
Moiety formula	C49 H69 Co2 N3 O7	C49 H69 Co2 N3 O7	
Sum formula	C49 H69 Co2 N3 O7	C49 H69 Co2 N3 O7	
Mr	929.93	929.93	
Dx,g cm-3	1.301	1.301	
Z	4	4	
Mu (mm-1)	0.751	0.751	
F000	1976.0	1976.0	
F000'	1979.49		
h,k,lmax	14,28,31	14,28,31	
Nref	13241	11671	
Tmin,Tmax	0.766,0.825	0.772,0.875	
Tmin'	0.766		

Correction method= GAUSSIAN

Data completeness= 0.881

Theta(max)= 29.500

R(reflections)= 0.0365(9819)

wR2(reflections)= 0.0946(11671)

S = 1.033

Npar= Npar = 574

The following ALERTS were generated. Each ALERT has the format

test-name_ALERT_alert-type_alert-level.

Click on the hyperlinks for more details of the test.

● Alert level G

PLAT005_ALERT_5_G	No	_iucr_refine_instructions_details	in the CIF	Please Do !
PLAT710_ALERT_4_G	Delete	1-2-3 or 2-3-4	Linear Torsion Angle ... #	27 Do !
	O1	-CO1 -N3 -C11	-17.10 0.50 1.555 1.555 1.555 1.555	
PLAT710_ALERT_4_G	Delete	1-2-3 or 2-3-4	Linear Torsion Angle ... #	28 Do !
	O1	-CO1 -N3 -C15	163.90 0.40 1.555 1.555 1.555 1.555	
PLAT710_ALERT_4_G	Delete	1-2-3 or 2-3-4	Linear Torsion Angle ... #	64 Do !
	O4	-CO1 -N2 -C9	41.00 0.50 1.555 1.555 1.555 1.555	
PLAT710_ALERT_4_G	Delete	1-2-3 or 2-3-4	Linear Torsion Angle ... #	65 Do !
	O4	-CO1 -N2 -C10	-127.90 0.40 1.555 1.555 1.555 1.555	
PLAT710_ALERT_4_G	Delete	1-2-3 or 2-3-4	Linear Torsion Angle ... #	79 Do !
	O6	-CO1 -O7 -C49	143.70 0.30 1.555 1.555 1.555 1.555	
PLAT710_ALERT_4_G	Delete	1-2-3 or 2-3-4	Linear Torsion Angle ... #	88 Do !
	O7	-CO1 -O6 -C48	152.40 0.30 1.555 1.555 1.555 1.555	
PLAT710_ALERT_4_G	Delete	1-2-3 or 2-3-4	Linear Torsion Angle ... #	105 Do !
	N2	-CO1 -O4 -CO2	-60.50 0.40 1.555 1.555 1.555 1.555	
PLAT710_ALERT_4_G	Delete	1-2-3 or 2-3-4	Linear Torsion Angle ... #	106 Do !
	N2	-CO1 -O4 -C46	93.00 0.40 1.555 1.555 1.555 1.555	
PLAT710_ALERT_4_G	Delete	1-2-3 or 2-3-4	Linear Torsion Angle ... #	113 Do !
	N3	-CO1 -O1 -CO2	-154.70 0.40 1.555 1.555 1.555 1.555	
PLAT710_ALERT_4_G	Delete	1-2-3 or 2-3-4	Linear Torsion Angle ... #	114 Do !
	N3	-CO1 -O1 -C1	-1.60 0.50 1.555 1.555 1.555 1.555	

0 **ALERT level A** = Most likely a serious problem - resolve or explain
0 **ALERT level B** = A potentially serious problem, consider carefully
0 **ALERT level C** = Check. Ensure it is not caused by an omission or oversight
11 **ALERT level G** = General information/check it is not something unexpected

0 ALERT type 1 CIF construction/syntax error, inconsistent or missing data
0 ALERT type 2 Indicator that the structure model may be wrong or deficient
0 ALERT type 3 Indicator that the structure quality may be low
10 ALERT type 4 Improvement, methodology, query or suggestion
1 ALERT type 5 Informative message, check

Datablock: NiZn-OH

Bond precision: C-C = 0.0027 A

Wavelength=1.54184

Cell: a=14.4458(3) b=19.0800(2) c=17.1363(2)
alpha=90 beta=106.3562(17) gamma=90
Temperature: 100 K

	Calculated	Reported
Volume	4532.06(12)	4532.04(11)
Space group	P 21/c	P 1 21/c 1
Hall group	-P 2ybc	-P 2ybc
Moiety formula	C45 H59 N3 Ni O4 Zn, C2 H4 C12	C45 H59 N3 Ni O4 Zn, C2 H4 C12
Sum formula	C47 H63 Cl2 N3 Ni O4 Zn	C47 H63 Cl2 N3 Ni O4 Zn
Mr	928.98	928.98
Dx,g cm-3	1.362	1.362
Z	4	4
Mu (mm-1)	2.606	2.606
F000	1960.0	1960.0
F000'	1948.97	
h,k,lmax	17,23,21	17,23,21
Nref	9168	9000
Tmin,Tmax	0.572,0.950	0.550,0.949
Tmin'	0.379	

Correction method= GAUSSIAN

Data completeness= 0.982 Theta(max)= 73.790

R(reflections)= 0.0324(8021) wR2(reflections)= 0.0888(9000)

S = 1.031 Npar= Npar = 559

The following ALERTS were generated. Each ALERT has the format

test-name_ALERT_alert-type_alert-level.

Click on the hyperlinks for more details of the test.

Alert level G

PLAT005_ALERT_5_G	No _iucr_refine_instructions_details	in the CIF	Please Do !
PLAT232_ALERT_2_G	Hirshfeld Test Diff (M-X)	Ni1 -- N2 ..	6.7 su
PLAT232_ALERT_2_G	Hirshfeld Test Diff (M-X)	Ni1 -- N3 ..	6.7 su
PLAT302_ALERT_4_G	Anion/Solvent Disorder Percentage =	100 Note
PLAT303_ALERT_2_G	Full Occupancy H-Atom	H4 with # Connections	2.00 Check
PLAT710_ALERT_4_G	Delete 1-2-3 or 2-3-4	Linear Torsion Angle ... #	40 Do !
	O1 -Ni1 -N3 -C10	166.00 21.00 1.555 1.555 1.555	1.555
PLAT710_ALERT_4_G	Delete 1-2-3 or 2-3-4	Linear Torsion Angle ... #	41 Do !
	O1 -Ni1 -N3 -C14	-16.00 5.00 1.555 1.555 1.555	1.555
PLAT710_ALERT_4_G	Delete 1-2-3 or 2-3-4	Linear Torsion Angle ... #	84 Do !
	O4 -Ni1 -N2 -C8	95.60 1.10 1.555 1.555 1.555	1.555
PLAT710_ALERT_4_G	Delete 1-2-3 or 2-3-4	Linear Torsion Angle ... #	85 Do !
	O4 -Ni1 -N2 -C9	-85.00 1.10 1.555 1.555 1.555	1.555
PLAT710_ALERT_4_G	Delete 1-2-3 or 2-3-4	Linear Torsion Angle ... #	90 Do !
	N2 -Ni1 -O4 -ZN1	-92.30 1.10 1.555 1.555 1.555	1.555
PLAT710_ALERT_4_G	Delete 1-2-3 or 2-3-4	Linear Torsion Angle ... #	95 Do !

N3 -Ni1 -O1 -ZN1 5.00 5.00 1.555 1.555 1.555 1.555
 PLAT710_ALERT_4_G Delete 1-2-3 or 2-3-4 Linear Torsion Angle ... # 96 Do !
 N3 -Ni1 -O1 -C1 -151.00 5.00 1.555 1.555 1.555 1.555
 PLAT860_ALERT_3_G Number of Least-Squares Restraints 5 Note

0 **ALERT level A** = Most likely a serious problem - resolve or explain
 0 **ALERT level B** = A potentially serious problem, consider carefully
 0 **ALERT level C** = Check. Ensure it is not caused by an omission or oversight
 13 **ALERT level G** = General information/check it is not something unexpected

0 ALERT type 1 CIF construction/syntax error, inconsistent or missing data
 3 ALERT type 2 Indicator that the structure model may be wrong or deficient
 1 ALERT type 3 Indicator that the structure quality may be low
 8 ALERT type 4 Improvement, methodology, query or suggestion
 1 ALERT type 5 Informative message, check

Datablock: NiNi-OMe

Bond precision: C-C = 0.0032 A Wavelength=1.54184

Cell: a=20.8266(6) b=13.0162(3) c=18.9697(4)
 alpha=90 beta=110.255(3) gamma=90

Temperature: 100 K

	Calculated	Reported
Volume	4824.4(2)	4824.4(2)
Space group	P 21/c	P 1 21/c 1
Hall group	-P 2ybc	-P 2ybc
Moiety formula	C48 H69 N3 Ni2 O6, C H4 O	C48 H69 N3 Ni2 O6, C H4 O
Sum formula	C49 H73 N3 Ni2 O7	C49 H73 N3 Ni2 O7
Mr	933.48	933.52
Dx,g cm-3	1.285	1.285
Z	4	4
Mu (mm-1)	1.378	1.378
F000	2000.0	2000.0
F000'	1980.93	
h,k,lmax	25,16,23	25,16,23
Nref	9732	9558
Tmin,Tmax	0.773,0.857	0.677,1.000
Tmin'	0.699	

Correction method= MULTI-SCAN

Data completeness= 0.982 Theta(max)= 73.580

R(reflections)= 0.0413(8295) wR2(reflections)= 0.1212(9558)

S = 1.043 Npar= Npar = 579

The following ALERTS were generated. Each ALERT has the format

test-name_ALERT_alert-type_alert-level.

Click on the hyperlinks for more details of the test.

Alert level B

Crystal system given = monoclinic

PLAT355_ALERT_3_B Long O-H (X0.82,N0.98A) O5 - H5 ... 1.08 Ang.

Alert level C

PLAT355_ALERT_3_C Long O-H (X0.82,N0.98A) O6 - H6 ... 1.03 Ang.

Alert level G

PLAT005_ALERT_5_G No _iucr_refine_instructions_details in the CIF Please Do !

PLAT710_ALERT_4_G Delete 1-2-3 or 2-3-4 Linear Torsion Angle ... # 75 Do !

O5 -N11 -O6 -C48 147.40 0.50 1.555 1.555 1.555 1.555

PLAT710_ALERT_4_G Delete 1-2-3 or 2-3-4 Linear Torsion Angle ... # 84 Do !

O6 -N11 -O5 -C47 147.80 0.50 1.555 1.555 1.555 1.555

- 0 **ALERT level A** = Most likely a serious problem - resolve or explain
- 1 **ALERT level B** = A potentially serious problem, consider carefully
- 1 **ALERT level C** = Check. Ensure it is not caused by an omission or oversight
- 3 **ALERT level G** = General information/check it is not something unexpected

- 0 ALERT type 1 CIF construction/syntax error, inconsistent or missing data
 - 0 ALERT type 2 Indicator that the structure model may be wrong or deficient
 - 2 ALERT type 3 Indicator that the structure quality may be low
 - 2 ALERT type 4 Improvement, methodology, query or suggestion
 - 1 ALERT type 5 Informative message, check
-

It is advisable to attempt to resolve as many as possible of the alerts in all categories. Often the minor alerts point to easily fixed oversights, errors and omissions in your CIF or refinement strategy, so attention to these fine details can be worthwhile. In order to resolve some of the more serious problems it may be necessary to carry out additional measurements or structure refinements. However, the purpose of your study may justify the reported deviations and the more serious of these should normally be commented upon in the discussion or experimental section of a paper or in the "special_details" fields of the CIF. checkCIF was carefully designed to identify outliers and unusual parameters, but every test has its limitations and alerts that are not important in a particular case may appear. Conversely, the absence of alerts does not guarantee there are no aspects of the results needing attention. It is up to the individual to critically assess their own results and, if necessary, seek expert advice.

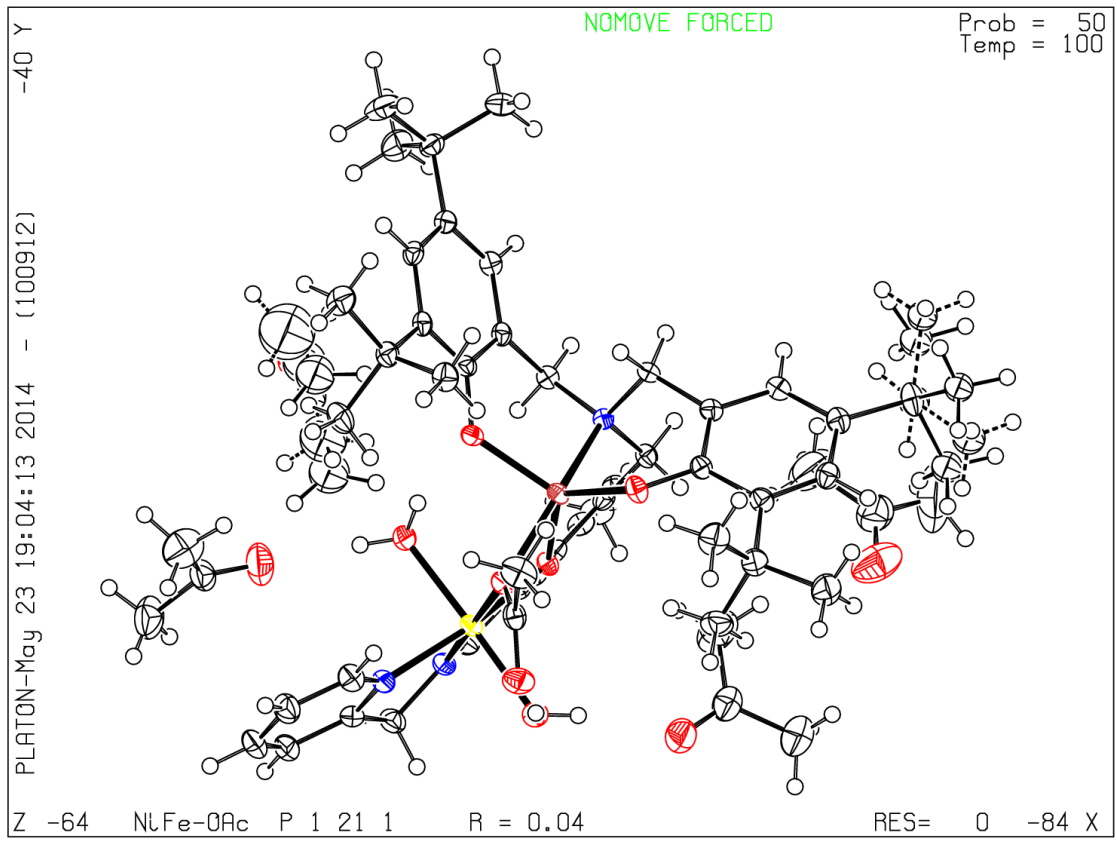
Publication of your CIF in IUCr journals

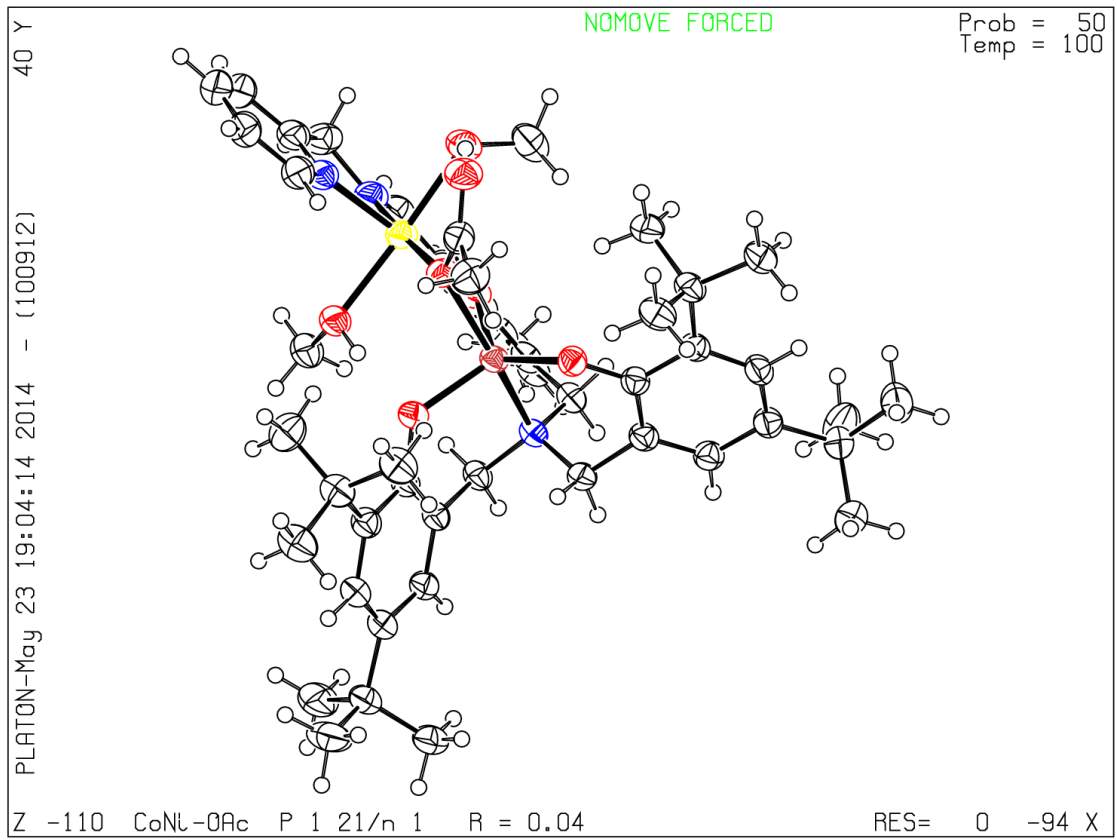
A basic structural check has been run on your CIF. These basic checks will be run on all CIFs submitted for publication in IUCr journals (*Acta Crystallographica*, *Journal of Applied Crystallography*, *Journal of Synchrotron Radiation*); however, if you intend to submit to *Acta Crystallographica Section C* or *E*, you should make sure that full publication checks are run on the final version of your CIF prior to submission.

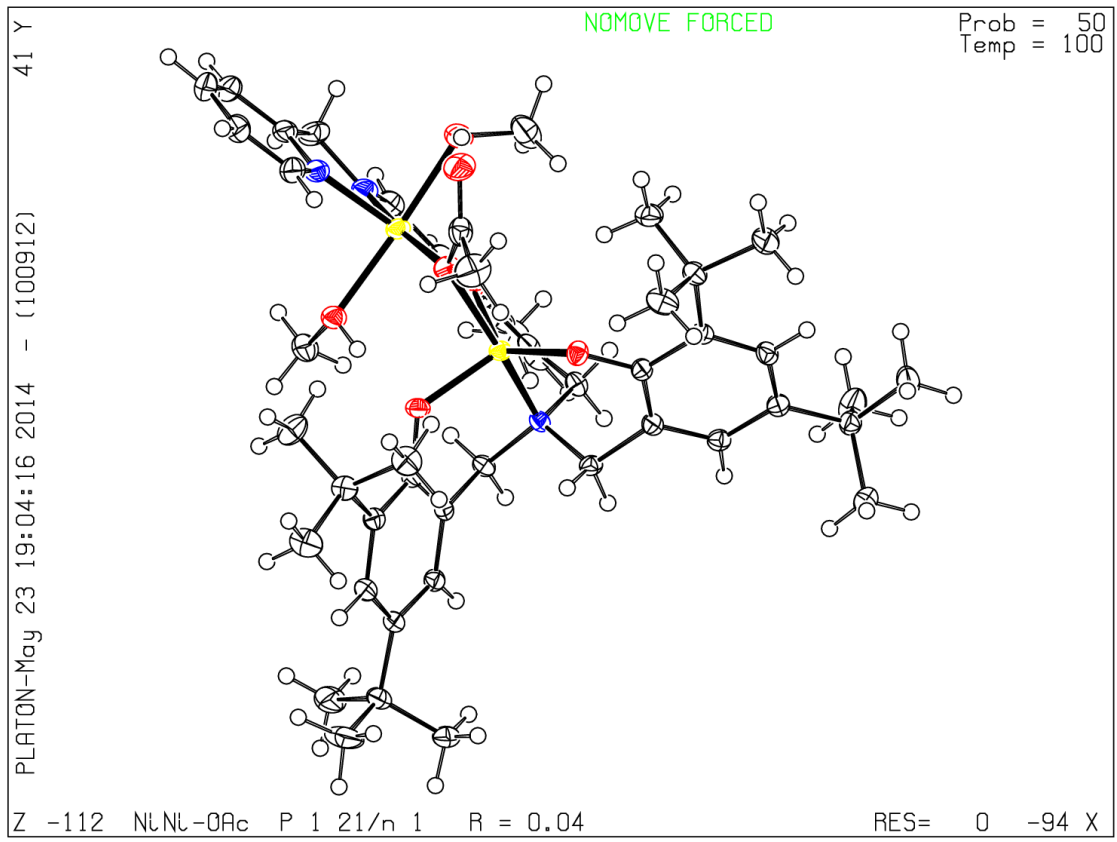
Publication of your CIF in other journals

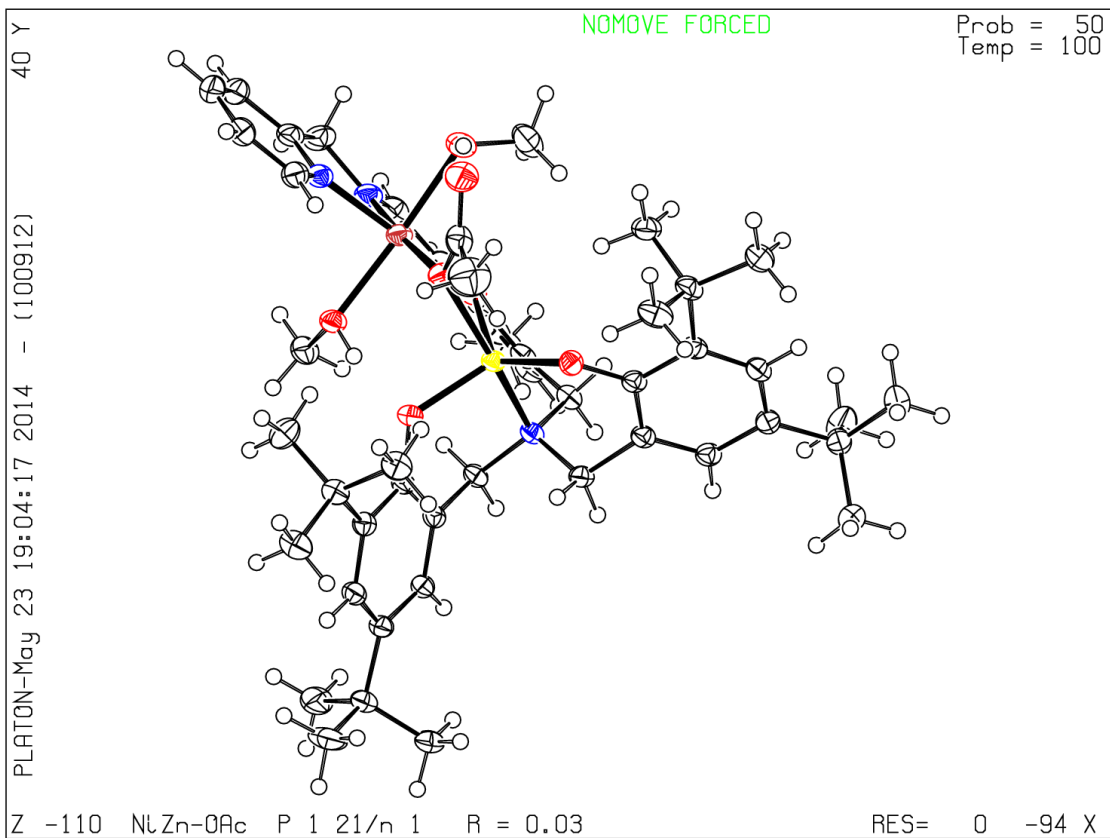
Please refer to the *Notes for Authors* of the relevant journal for any special instructions relating to CIF submission.

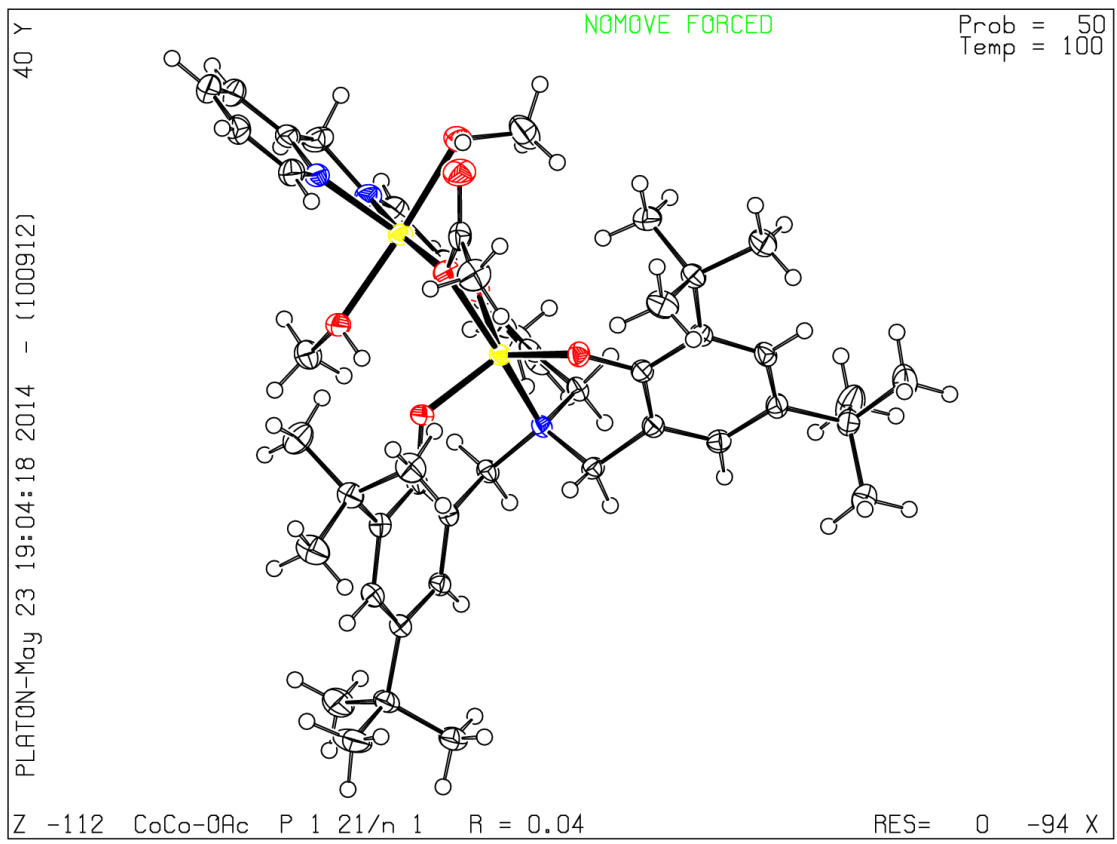
PLATON version of 05/02/2014; check.def file version of 05/02/2014

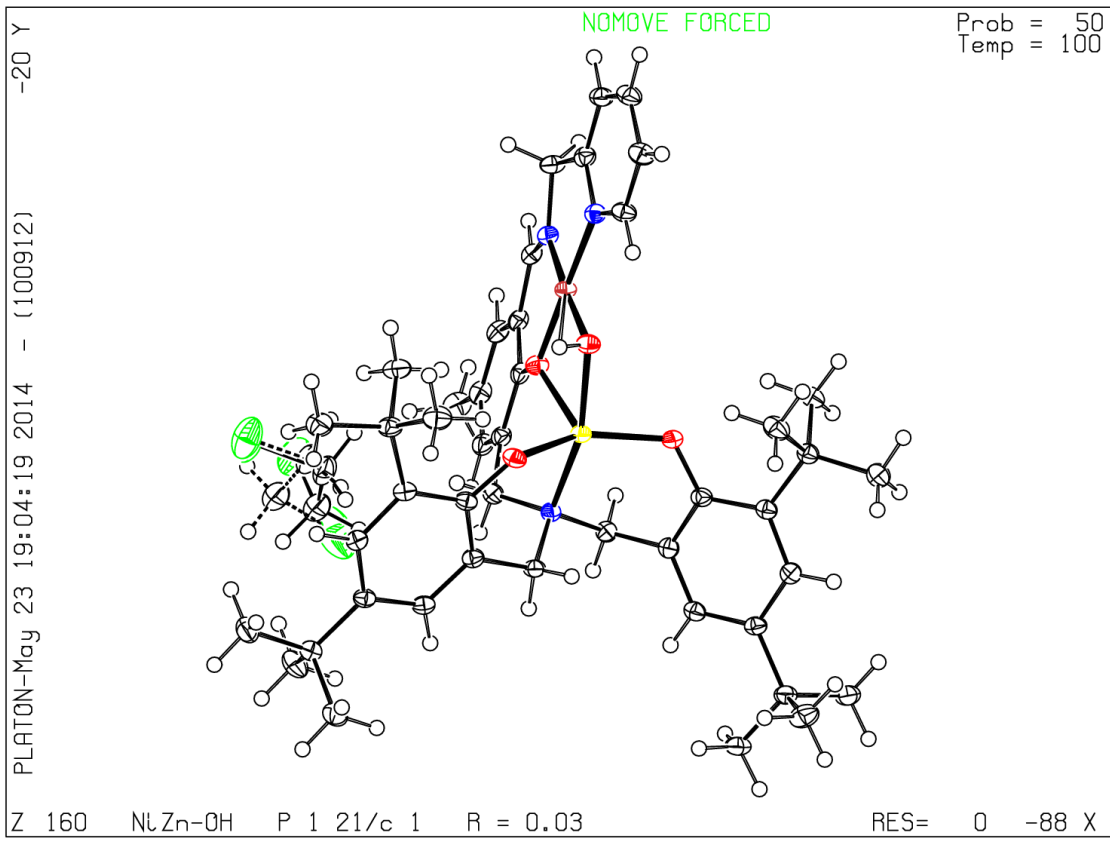


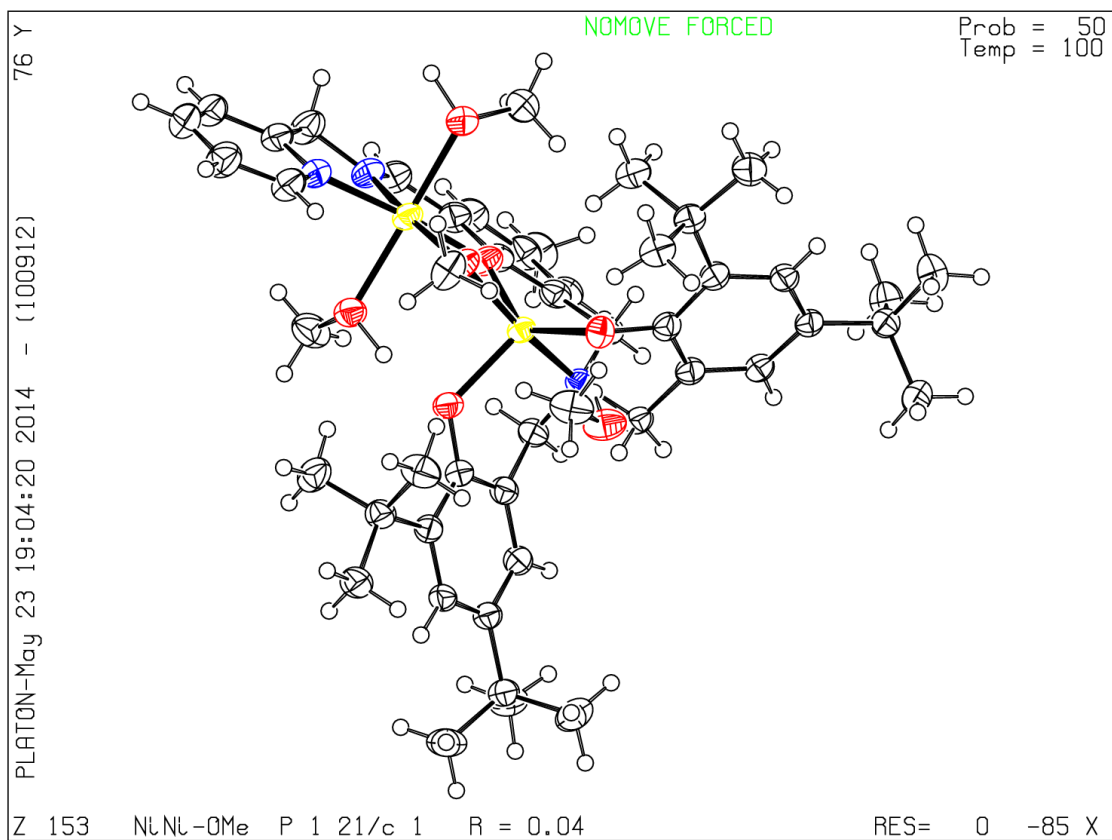












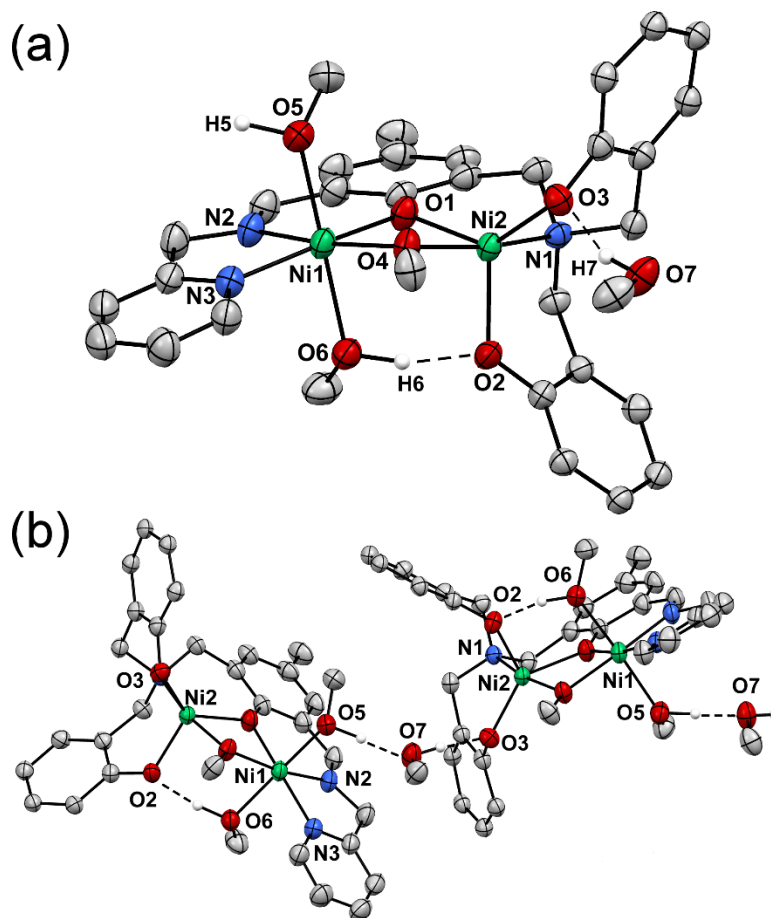


Figure S1. Thermal ellipsoid plots (50% probability) derived from the X-ray structure of NiNi^{OMe} . Most hydrogen atoms and the *tert*-butyl substituents of the terminal phenolate donors have been removed for clarity. Figure S1(a) shows only the NiNi^{OMe} unit, while (b) displays the two hydrogen-bonds formed by each MeOH solvate: $\text{O}(5)\text{-H}\cdots\text{O}(7)$ and $\text{O}(7)\text{-H}\cdots\text{O}(3)$.

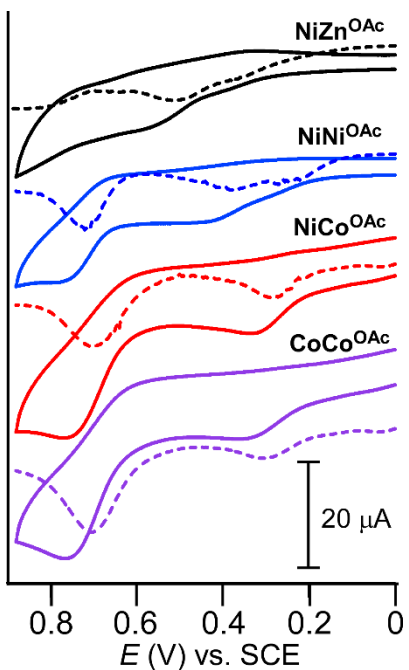


Figure S2. Cyclic voltammograms (solid lines) of NiZn^{OAc} , NiNi^{OAc} , NiCo^{OAc} , and CoCo^{OAc} collected in DMF with 0.1 M $(\text{NBu}_4)\text{PF}_6$ as the supporting electrolyte and scan rates of 100 mV/s. The corresponding square-wave voltammograms are indicated by the dashed lines. In all cases the voltammogram was initiated by the anodic sweep. The solution concentrations were 2.0 mM.